THE EFFECTS OF IMMOBILIZATION ON STRUCTURE AND SUBSTRATE ACTIVATION OF GLUTAMATE DEHYDROGENASE

Thesis by

Kim Claire O'Connor

In Partial Fulfillment of the Requirements

for the Degree of

Doctor of Philosophy

California Institute of Technology

Pasadena, California

1987

Submitted April 17, 1987

© 1987

Kim Claire O'Connor

All Rights Reserved

This doctoral thesis
is dedicated
with *love*
to my mother,
Mrs. Doris Julia O'Connor.

Wisdom is glorious, and never fadeth away,
and is easily seen by them that love her,
and is found by them that seek her.

— THE OLD TESTAMENT
Wisdom, 6: 13

Acknowledgments

This doctoral thesis was made possible by the support of my teachers and benefactors.

During my academic training at Duchesne Academy of the Sacred Heart, Rice University and Caltech, I was taught by many gifted individuals who shared with me their knowledge, love for learning and dedication to their craft. For this, I am very grateful. Of these people, I would like to recognize the members of my thesis review committee (Drs. Frances Arnold, James Bailey, Sunney Chan and George Gavalas) for their interest in my graduate research and my career in bioengineering. In addition, I am grateful to Dr. Chan for giving me unlimited access to his ESR spectrophotometer and for reviewing my paper on ketone-labeled glutamate dehydrogenase prior to publication. Mr. Steve Witt at Caltech taught me how to operate the ESR spectrophotometer and provided me with computer programs to analyze spectra. His efforts are greatly appreciated. Finally and most importantly, I would like to thank my advisor, Dr. Bailey, for introducing me to biochemical engineering, giving me the freedom to pursue my research interests, advising me on my research and future career plans, and providing me with financial support.

Several foundations have sponsored my academic training. At Rice University, I was a Robert A. Welch Merit Scholar, Brown Engineering Merit Scholar

and Roy Merit Scholar. My first year at Caltech was sponsored by the Weyerhaeuser Company Foundation, and my graduate research was funded by the National Science Foundation. I am extremely grateful to all of these foundations for their generosity.

Abstract

Structure and substrate activation of bovine liver glutamate dehydrogenase were investigated when the enzyme was in its native state or was covalently bound via primary amino groups to a solid Sepharose bead. In this research, the enzyme was covalently bound directly to CNBr-activated Sepharose 4B or indirectly, via a six-carbon spacer arm, to CH-activated Sepharose 4B. Electron spin resonance spectroscopy was employed to study structure. This study required spin labeling glutamate dehydrogenase with either 2,2,6,6-tetramethyl-4-oxopiperidine-1-oxyl or 4-((4-(chloromercurio)benzoyl)amino)-2,2,6,6-tetramethyl-1-piperidinyloxy. Substrate activation of the deamination of glutamate by NAD was visible in Lineweaver-Burk plots of inverse rate vs. inverse substrate concentration.

The electron spin resonance spectrum of glutamate dehydrogenase spin labeled with 2,2,6,6-tetramethyl-4-oxopiperidine-1-oxyl was a composite consisting primarily of two populations of spin labels with outer peak separations of 33 gauss (population A) and 69 gauss (population B). For the native enzyme in solution, population A accounted for 10% of the spectrum. This percentage increased to 21 when the active site was saturated with substrates during spin labeling and increased to 34 when the enzyme was immobilized to either CNBr- or CH-activated Sepharose. The roles of aspecific labeling and structural heterogeneity in these spectral changes were discussed. Modification of the native and immobilized enzyme with pyridoxal 5'-phosphate characterized the binding

site(s) for the spin label. Deconvolution of experimental spectra into populations A and B divulged a subpopulation of labels with a mobility unlike those of the two principal components. Linear combinations of the deconvoluted line shapes for populations A and B successfully represented all spectra of glutamate dehydrogenase from this and previous investigations.

Conformational change in glutamate dehydrogenase was investigated by spin labeling the enzyme at cysteine 319 with 4-((4-(chloromercurio)benzoyl)-amino)-2,2,6,6-tetramethyl-1-piperidinyloxy. Electron spin resonance spectra of spin-labeled glutamate dehydrogenase showed that immobilization of the enzyme on CNBr-activated Sepharose 4B suppressed conformational change induced by GTP and NADPH and profoundly altered that induced by α-ketoglutarate. Moreover, the spectrum of the immobilized enzyme provides evidence for structural heterogeneity at cysteine 319.

Covalently binding glutamate dehydrogenase to CNBr- and CH-activated Sepharose 4B altered the substrate activation pattern of the biocatalyst. Specifically, the sharp discontinuity, which characterizes Lineweaver-Burk plots of free enzyme kinetics with NAD as the varied substrate, became elongated when the biocatalyst was attached to either support. The elongated transition region contains two inflection points and resembles substrate activation of several other allosteric oligomers. Under the same experimental conditions, glutamate induced varying degrees of abrupt activation in immobilized glutamate dehydrogenase and inhibited the enzyme in solution. The intensity of this activation is inversely proportional to the rate constant of the biocatalyst-Sepharose conjugate. These modified activation patterns may be due in part to increased

structural heterogeneity and altered conformational change. The above kinetic results are free of mass transport effects: the external effectiveness factor was unity, the observable Thiele modulus was less than $2.0 \cdot 10^{-4}$, and reaction-generated pH change was less than 0.01 for all data reported in this paper.

Table of Contents

List of Figures

List of Tables

Nomenclature

a	external surface area per volume of bead (cm^{-1})
A_B	bead area (cm^2)
ClHgBz-TEMPO	4-((4-(chloromercurio)benzoyl)amino)
	-2,2,6,6-tetramethyl-1-piperidinyloxy
D	diffusion coefficient (cm^2/sec)
D_a	Damköhler number (dimensionless)
e_f	functional protomer
ESR	electron spin resonance
G	mass velocity (g/cm^2 per sec)
GluDH	glutamate dehydrogenase
k_{app}	apparent rate constant (mole NADH/mole e_f per min)
k_S	mass transfer coefficient for S (cm/sec)
$K_{m,\,app}$	apparent Michaelis-Menten dissociation constant (mM)
K	dissociation constant (mM or M)
N_{Re}	Reynolds number (dimensionless)
n	number of species
N_{Sc}	Schmidt number (dimensionless)
R	bead radius (μm)
S	substrate
v	initial steady state velocity (mole NADH/ml per min)
V	molar volume (ml/mole)

V_B bead volume (cm^3)

X, X' chemical species

y extent of reaction (M)

Greek

δ extent of association (M)

ϵ_B bed porosity (dimensionless)

η_e external effectiveness factor (dimensionless)

μ viscosity (g/cm per sec)

ν stoichiometric coefficient (dimensionless)

ρ fluid density (g/ml)

ϕ's kinetic parameters

Φ observable Thiele modulus (dimensionless)

Superscripts and subscripts

G glutamate

i ith species

N NAD

o observable

$pore$ within bead

r position variable (μm)

INTRODUCTION

Industrial and medical applications of enzymes require that these enzymes be functional in process conditions far different from their natural surroundings. The functional properties, as well as the structural properties, of an enzyme change when the enzyme is moved from its natural surroundings to an artificial environment [1,2,3]. This research focuses on characterizing these changes and understanding the relationship between enzyme structure and function. This knowledge will enable the bioengineer to optimize enzyme function in a particular set of process conditions.

Today, enzymes are employed in a variety of industrial and medical processes: lipase degrades fats in waste treatment facilities, protease is a component of many detergents, asparaginase is an anticancer agent, and glucose isomerase is used in the production of fructose-glucose syrups from corn starch. These four examples are just a small sample of the current applications of enzymes given in References 4 and 5.

To date, investigators have primarily employed monomers in their studies of enzymes in artificial environments [1,2,3]. Numerous industrial applications involving allosteric oligomers [5] necessitate that more research be done in this area. To this end, the research described within compares the structural and functional properties of bovine liver glutamate dehydrogenase (GluDH, EC 1.4.1.3), a hexamer, when this enzyme is covalently coupled (or immobilized) to a solid Sepharose support to when it is dissolved (or free) in an aqueous solution. In addition, this research examines the relationship between these properties. GluDH was chosen for this work because it is representative of a variety of allosteric enzymes which are regulated by NAD(P), ADP and GTP. For

example, glyceraldehyde 3-phosphate dehydrogenase from lobster muscle, alcohol dehydrogenase from horse liver, lactate dehydrogenase from dog-fish, and GluDH from *Neurospora* and bovine liver have a common secondary structure of six parallel β-sheets which forms a NAD(P) binding domain [6]. The Sepharose support was chosen as the artificial environment in which to study the enzyme since GluDH immobilized to CNBr-activated Sepharose 4B is used by the medical community to synthesize ^{13}N-labeled amino acids as imaging agents for bone tumors, heart, pancreas and brain by positron-emission tomography [7,8].

An important advantage in working with GluDH is that it provides the investigator with several structure-function relationships from which to choose a research project. ADP, an activator, and GTP, and inhibitor, may regulate activity by inducing conformational change in GluDH. Such change has been detected with electron spin resonance (ESR) spectroscopy [9]. Likewise, these effectors may act by altering the degree to which the hexamers aggregate [10]. In the presence of NADH and GTP, the rate at which α-ketoglutarate is aminated increases during the time course of the reaction. This activation may be triggered through subunit interactions when half of the coenzyme binding sites are occupied by NAD [11]. In the absence of effectors, NAD(P) activates the deamination of glutamate [12]. A kinetic model of this activation suggests that this phenomenon can be caused by structural heterogeneity, conformational change or a second NAD(P) binding site per subunit of the hexamer [13].

All of the above mentioned structure-function relationships that involve effectors, ADP and GTP, are a composite of two such relationships: one involves the effector; the other, substrates whose reaction the effector regulates. Thus,

structure-function relationships associated with substrates must be fully understood before the same can be said of those relationships associated with ADP and GTP. Information on the former is incomplete. The roles of structural heterogeneity and a second NAD(P) binding site per subunit in substrate activation have only been predicted in a kinetic model [13]. To date, there are no data to support or to dispute this claim. Data showing substrate-induced conformational change in GluDH are available [9]; however, the role that this change plays in substrate activation is not completely clear. Because of this, the research described within focuses on substrate activation rather than effector regulation.

Since the role of GluDH structure in substrate activation is not fully understood, the original objective of comparing the properties of immobilized GluDH to those of the free enzyme was expanded to include investigating structure-function relationships associated with substrate activation. In this work, immobilization was used to investigate these relationships. As this research demonstrates, immobilization exaggerates structural and kinetic features of GluDH which makes patterns of change and relationships more detectable than in the free enzyme. Others have used immobilization to study allosteric regulation of oligomeric proteins. For example, the effects of artificial conformational constraints on the affinity of hemoglobin for O_2 were investigated by crosslinking the oligomer into a glutaraldehyde membrane [14]. ADP and GTP regulation were studied in GluDH that had been absorbed onto two types of supports containing spacer arms: palmityl- and Triton X-100-substituted Sepharose 4B [15,16]. In these investigations, only protein function was monitored. In this research, structure is also examined. By measuring both protein structure and function,

more insight into allosteric regulation can be achieved than by monitoring only one of these properties.

In this investigation, GluDH structure was studied with ESR spectroscopy. In its natural state, the enzyme does not emit an ESR signal; however, a paramagnetic spin label covalently attached to GluDH enables the investigator to examine the structure of the enzyme. Specifically, the structure is reflected in the label's rotational freedom around the bond which fastens the label to the enzyme [17]. ESR spectroscopy was chosen over other methods, such as circular-dichroism, because it focuses on the local environment of the spin label rather than the entire enzyme molecule. In this way, small changes in structure could be observed that would go undetected using a method that is more global in nature.

This study of structure and substrate activation in free and immobilized GluDH is presented in three chapters. Chapters 1 and 2 concern ESR spectroscopy studies of the enzyme, while chapter 3 contains the kinetic investigations of substrate activation. Each chapter is divided into the following sections: Introduction, Materials and Methods, Comments (chapter 3 only), Results, Discussion, Footnotes (chapters 1 and 3 only), References, Tables (chapters 1 and 3 only), and Figures. For the reader's convenience, specific conclusions from each chapter are summarized in the "Concluding Remarks" at the end of this thesis.

References

1 Cambou, B. and Klibanov, A. M. (1984) J. Am. Chem. Soc. 106, 2687-2692

2 Yoshimoto, T., Takahashi, K., Nishimura, H., Ajima, A., Tamaura, Y. and Inada, Y. (1984) Biotechnol. Lett. 6, 337-340

3 Clark, D. S. and Bailey, J. E. (1983) Biotechnol. Bioeng. 25, 1027-1047

4 Bailey, J. E. and Ollis, D. F. (1977) Biochemical Engineering Fundamentals, pp. 155-215, McGraw-Hill, New York

5 Godfrey, T. and Reichelt, J. (1983) Industrial Enzymology, Nature Press, New York

6 Wootton, J. C. (1974) Nature 252, 542-546

7 Cooper, A. J. L. and Gelbard, A. S. (1981) Anal. Biochem. 111, 42-48

8 Gelbard, A. S., Benua, R. S., Reimam, R. E., McDonald, J. M., Vomero, J. J. and Laughlin, J. S. (1980) J. Nucl. Med. 21, 988-991

9 Zantema, A., Vogel, H. J. and Robillard, G. T. (1979) Eur. J. Biochem. 96, 453-463

10 Sund, H., Markau, K. and Koberstein, R. (1975) in Biological Macromolecules, Subunits in Biological Systems, Part C, vol. 7 (Timasheff, S. N. and Fasman, G. D., eds.), pp. 225-287, Marcel Dekker, New York

11 Smith, T. and Bell, J. E. (1982) Biochemistry 21, 733-737

12 Engel, P. C. and Dalziel, K. (1969) Biochem. J. 115, 621-631

13 Engel, P. C. and Ferdinand, W. (1973) Biochem. J. 131, 97-105

14 Guillochon, D., Bourdillon, C. and Thomas, D. (1978) Enzyme Eng. 4, 373-379

15 Nemat-Gorgani, M. and Karimian, K. (1983) Biotechnol. Bioeng. 25, 2617-2629

16 Nemat-Gorgani, M. and Karimian, K. (1984) Biotechnol. Bioeng. 26, 565-572

17 Morrisett, J. D. (1976) in Spin Labeling: Theory and Applications (Berliner, L. J., ed.), pp. 273-338, Academic Press, New York

CHAPTER 1

An ESR Spectroscopy Study of Free and Immobilized Glutamate Dehydrogenase Spin Labeled with 2,2,6,6-Tetramethyl-4-Oxopiperidine-1-Oxyl

Introduction

Bovine liver GluDH catalyzes the reversible deamination of L-glutamate and, to a lesser degree, other amino acids by NAD(P) [1,2]. The smallest enzymatically active unit of GluDH is a hexamer with a molecular weight of 336 000. Each of the six GluDH polypeptide chains, called protomers, has the same amino acid sequence and a molecular weight of 56 000. Furthermore, each protomer has an active site and regulatory sites for NAD(P), ADP and GTP [3]. Hucho and Janda have shown with crosslinking reagents and electrophoresis that these protomers are arranged in two layers of three trimers [4]. In this quaternary structure, GluDH has different conformations. For example, ESR spectra reveal that structural change occurs when amino acid substrates, NAD(P)H, ADP and GTP bind to the enzyme [5]. These and other properties of this allosteric oligomer are summarized by Sund, Markau and Koberstein [3].

Currently, GluDH is utilized in process conditions far different from its natural surroundings. In medical laboratories, this hexamer is immobilized on CNBr-activated Sepharose 4B to synthesize ^{13}N-labeled L-amino acids as imaging agents for bone tumors, heart, pancreas and brain by positron-emission tomography [6,7]. In general, the properties of an enzyme, such as activity and structure, are modified when the enzyme is exposed to artificial environments, like immobilization [8,9]. This necessitates fundamental research of these properties in the particular operating conditions where the enzyme is being utilized. To this end, this work examines structural changes in GluDH induced by binding the enzyme directly to CNBr-activated Sepharose 4B or via a six-carbon spacer arm to CH-activated Sepharose 4B.

In this ESR study, the surface structure of GluDH was investigated by spin labeling the enzyme with 2,2,6,6-tetramethyl-4-oxopiperidine-1-oxyl. This ketone spin label covalently binds to GluDH at a primary amino group after an $NaBH_4$ reduction of an intermediate Schiff base [10]. This reaction deactivates the enzyme [11]. Previous studies with this ketone label have generated ESR spectra of free GluDH with different overall line shapes [11,12,13]. One of these line shapes was obtained in this research, and two new spectra were generated. Reasons for these spectral changes are discussed in this paper.

Materials and methods

Chemicals and equipment

Pharmacia supplied CNBr- and CH-activated Sepharose 4B. Bovine liver glutamate dehydrogenase suspended in a 50% glycerol solution was purchased from Boehringer Mannheim Biochemicals along with the company's purest preparations of α-ketoglutarate, NAD and NADH. Polyethylene glycol (mwt 40 000) was distributed by Serva. Aldrich produced the dioxane (gold-label grade) and 2,2,6,6-tetramethyl-4-oxopiperidine-1-oxyl. Glutamate, fluorescein isothiocyanate and pyridoxal 5'-phosphate of the highest purity available were obtained from Sigma. All other chemicals were analytical grade reagents. Distilled, deionized water was used in all experiments.

The ultrafiltration cell that was utilized in the immobilization and rate assays contained Millipore's 13 mm, Swinnex filter unit made of polypropylene. This unit included a cellulose filter with an average pore diameter of 8.0 μm. A 52×14 mm, cylindrical, polycarbonate extension barrel was used to expand the bed volume of the filter unit. (The barrel was discontinued by Millipore in 1975.) A Shimadzu double-beam UV-260 recording spectrophotometer with temperature control and data analysis was employed for concentration and rate measurements. End-over-end rotation was achieved with a Cole-Parmer variable-speed"Roto-torque" rotator. Spectra were recorded and analyzed on a Varian E-line Century Series X-Band ESR spectrometer connected to a Compac-Plus microcomputer.

The following buffers were used in this investigation: buffer 1, 87 mM sodium phosphate (pH 8.0); buffer 2, 87 mM sodium phosphate (pH 8.0) containing 10 μM EDTA; buffer 3, 0.15 M sodium phosphate (pH 8.0); buffer 4,

50 mM Tris/100 mM NaCl/0.1 mM EDTA (pH 7.4); and buffer 5, 50 mM sodium phosphate (pH 7.2).

Immobilization

The GluDH-glycerol solution was exhaustively dialyzed against buffer 1 at 4 °C. Centrifugation at 30 000 × g and 5 °C for 20 min followed. Next, 9 ml of the clarified liquid, containing from 1.5 (condition C in Table 1.2) to 5 mg/ml GluDH (condition B), was put in a 20 ml scintillation vial. (The concentration of GluDH was determined spectrophotometrically at 280 nm with an absorption coefficient of 0.93 $cm^{-1}mg^{-1}ml$ [5]. *In this work, one mole of enzyme is defined to be one mole protomer.*) While this enzyme sample was still at 4 °C, enough chilled dioxane was added to make the final solution contain 10% (v/v) of this anticoagulant. Throughout the remainder of this procedure, the protein sample was kept below 10 °C. At higher temperatures, dioxane precipitates the hexamer [14].

To prepare either CNBr-activated Sepharose (condition B in Table 1.2) or CH-activated Sepharose (condition C), the beads were washed with 200 ml/(g bead) of 1 mM HCl on the Swinnex filter unit containing the extension barrel. This was succeeded by a 200 ml/(g bead) wash with buffer 1. After the addition of 500 mg chilled Sepharose to the enzyme-dioxane solution, the heterogeneous mixture was rotated end-over-end at 13 rpm and 4 °C for 24 hr while the hexamer coupled to the support. After this time interval, the GluDH-Sepharose complex was washed with 2 l/(g bead) of buffer 1 at 4 °C on the ultrafilter to remove unreacted protein. (Usually Sepharose is washed with two buffers, one at pH 8.0 and the other at pH 4.0 [15]. Since the hexamer dissociates into protomers at pH 4.0, only a single buffer at pH 8.0 was

employed [16]. A greater volume of buffer 1 was used than required for the two-buffer wash to ensure complete removal of unreacted GluDH. This was verified with the free enzyme contamination test described in the next paragraph.) The immobilized hexamer was stored in buffer 1 at 4 °C and a concentration of 10 to 20 (mg bead)/ml.

To test for free enzyme contamination in immobilized GluDH, 4 mg of beads was assayed for kinetic activity as described below. After this sample was washed with 25 ml of buffer 2, its activity was reevaluated. The kinetic assay required an additional 25 ml of this buffer. This was repeated 13 times, exposing the immobilized GluDH sample to a total of 650 ml of buffer 2. During the entire procedure, the activity remained constant. Thus, the initial 2 l/(g bead) wash was sufficient to remove any unreacted protein.

Standard ketone labeling

The procedure outlined by Andree and Zantema [11] was modified for the immobilized enzyme. First, 200 mg of GluDH-Sepharose beads was washed with 20 ml of buffer 3 and filtered with the extended Swinnex system until the sample was damp. The beads were incubated with 10 ml of 140 mM ketone label in buffer 3. (The nitroxide dissolved slowly and left organic impurities. Before the immobilized hexamer was added to the ketone solution, Nalge's disposable filterware with a 0.2 μm pore diameter removed this residue.) The mixture was rotated end-over-end for 30 min at 25 °C. After this liquid was put on ice, a 2 fold molar excess of $NaBH_4$ over the ketone label was added slowly. The pH of the solution was maintained between 8 and 8.5 with 1.0 M HCl. After the reaction terminated (0.5 to 1 hr on ice), a second incubation followed: the sample was rotated end-over-end for 5 hr at 25 °C and then 17 hr at 4 °C.

At the end of this incubation period, the ketone solution was removed by filtration, and the beads were washed at 4 °C with 500 ml of buffer 1 to prepare the sample for activity measurements. At this point, the kinetics protocol was implemented. However, if the spin-labeled GluDH-Sepharose conjugate was intended for ESR analysis, it was washed with 250 ml of buffer 4 at 4 °C. Then, the sample was exposed to the same volume of buffer 4 recycling through the filter system. This was done at 4 °C for a total of three times: 4, 12 and 2 hr in length as described by Clark and Bailey [9]. Prior to recording the ESR spectrum, oxygen in the sample was purged by sparging this solution with N_2 (g); this prevented oxygen-nitroxide interactions which broaden a spectrum [17]. The spin-labeled beads were placed in a conical test tube containing 5 ml of buffer 4. After the tube was sealed with a septum, a 15 cm long, 19 G syringe needle injected N_2 into the sample for 2 hr at 4 °C. A standard, 23 G needle in the septum maintained a constant pressure. A slurry of degassed beads was transferred via a syringe from the sealed, conical tube to a quartz ESR tube with an 1.5 mm inner diameter.

For free GluDH, standard ketone labeling required incubating the enzyme with the ketone label for 30 min at 25°C prior to the $NaBH_4$ reduction and for 4.5 hr at 25°C followed by 18 hr at 4°C after the reduction. Andree's and Zantema's protocol was supplemented with the following techniques to spin label the free enzyme.

The initial GluDH-glycerol solution was concentrated at 4 °C from 5 to 15 mg/ml by enclosing the solution in a dialysis bag and by submerging the bag for 4 hr in a solution of buffer 3 containing 10 to 15% (w/v) polyethylene glycol. A highly polymerized form of polyethylene glycol with a molecular

weight of 40 000 was chosen. This prevented diffusion of the polymer into the enzyme solution through the dialysis membrane which had a molecular weight cutoff of 12 000.

The degassing system for immobilized GluDH was not applicable to the free enzyme; it caused foaming. The standard way to overcome this dilemma is to freeze the enzyme before introducing N_2 [17]. However, we found that freezing precipitates GluDH. These problems were circumvented by having a 2 ml sample of spin-labeled, free GluDH enclosed in a dialysis bag and submerged in 1 liter of buffer 4. N_2 was bubbled through the outer fluid for 2 hr at 4 °C. This allowed N_2 and O_2 to be exchanged across the dialysis membrane.

Unlike labeling immobilized GluDH, the solution containing the free enzyme foamed when reduced with $NaBH_4$. If any precipitate formed, the spin-labeled sample was centrifuged as described above. This prevented spectral contamination by denatured protein.

Substrate saturation

The ketone-labeling procedure given in the previous section was changed for substrate saturation. Prior to the thirty-minute incubation at 25 °C, enough NADH and α-ketoglutarate were added to the ketone solution to make it 3 mM and 16 mM, respectively. The reduced sample rotated end-over-end for 4 hr at 25 °C. This was followed by a dialysis against 100 mM α-ketoglutarate in buffer 4 for 4 hr at 4 °C.[1] Then, the spin-labeled enzyme was thoroughly dialyzed at the same temperature against buffer 4 to remove both the ketone label and substrates.

Recording and analyzing spectra

While acquiring the spectra, the recording parameters: scan range, field set, time constant, scan time, modulation frequency, gain, power and microwave frequency had corresponding values of 100 G, 3 400 G, 0.128 to 0.5 sec, 8 to 16 min, 100 kHz, $2.5 \cdot 10^4$ to $4.0 \cdot 10^5$, 5 mM and 9.5 GHz. The modulation amplitude was set to less than one-fourth to one-half of the narrowest peak-to-peak line width in gauss. For all spectra reported in this work, varying the instrument settings had no effect on the line shape. Also, saturation was avoided in all experiments [17]. All ESR curves were obtained at 25 °C.

Deconvoluted spectra, percentages of the mobile component (population A) in spectra, and spin label concentrations were all generated by processing ESR data on a microcomputer interfaced with the spectrometer. Spectra were resolved into their principal components (populations A and B) by subtracting and smoothing experimental curves. The fraction of "A" labels, f_A, in a sample was calculated by first reconstructing the experimental line shape, S_E, from the deconvoluted spectra for populations A and B, S_A and S_B.

$$S_E = mS_A + nS_B, \qquad m \;\&\; n = real\ numbers > 0. \tag{1.1}$$

The coefficients, m and n, were combined in the following manner with the second integrals, I_A and I_B, of the deconvoluted spectral curves to obtain f_A.

$$f_A = \frac{mI_A}{mI_A + nI_B}. \tag{1.2}$$

In this paper, all spectra are the first derivatives of their absorption curves. Thus, the second integral of a spectrum is proportional to the nitroxide concentration in the ESR sample [17].

The concentration of the ketone probe in an ESR sample was determined by recording the line shape of a known concentration of the unattached ketone label. The second integrals from the experimental curve and this control were compared after the latter was scaled to account for differences in recording parameters between the two [11,17].

Kinetics

Initial steady state GluDH velocities were measured spectrophotometrically at 340 nm and 25 °C in buffer 2 [1]. NADH formation for the free enzyme was assayed in 2 ml of this buffer containing 1 mM glutamate and 2 mM NAD. The reaction was initiated by adding 4 μg of GluDH. Ford et al. designed a recirculation reactor system for monitoring immobilized enzyme activity (Figure 1 of Reference 18). The extended Swinnex filter unit acted as the reactor. It was gradientless by maintaining the per pass conversion at less than 1.0% with a flow rate of 33 ml/min. The reactor was charged with 4 mg of beads. Then, the immobilized enzyme activity was measured in 25 ml of buffer 2 containing 10 mM glutamate and 2 mM NAD. Typical reaction rates for the free and immobilized GluDH assays were 20 and 200 (nmole NADH formed)/min, respectively. During deactivation experiments, the amount of free or immobilized enzyme assayed was increased to maintain the same reaction rate. For all free GluDH measurements, the enzyme concentration was sufficiently low that only active hexamers were present [19]. The molar absorption coefficient for NADH is 6.22 $mM^{-1}cm^{-1}$ at 340 nm [20]. Doubling the amount of free or immobilized enzyme had no effect on the activity on a per mass GluDH basis.

Chemical modification of free GluDH with pyridoxal 5'-phosphate

Pyridoxal 5'-phosphate was covalently bound to the free enzyme by the protocol given by Anderson and co-workers [21]. Their calculations were based on a molecular weight of 250 000 for GluDH. All concentrations were adjusted to the convention used here: a molecular weight of 56 000. Specifically, the initial GluDH-glycerol solution was thoroughly dialyzed at 4 °C against buffer 5. Centrifugation at 30 000 × g and 5 °C for 20 min followed. Next, 80 ml of 1 mg/ml GluDH in this buffer was mixed with an 11 fold molar excess of pyridoxal 5'-phosphate for 20 min at 34 °C. Any solution containing pyridoxal 5'-phosphate was kept in the dark since this compound is dimerized by light. After this incubation period, the modified GluDH solution was put on ice, and 4% (w/v) $NaBH_4$ in buffer 5 at 4 °C was injected under the solution surface until the molar ratio of $NaBH_4$ to pyridoxal 5'-phosphate was 6.6. The yellow liquid turned clear, indicating that all excess inactivator had been reduced [22]. The GluDH solution was mixed at 4 °C for 1 hr. This was succeeded by a 4 hr dialysis at 4 °C against 2 liters of buffer 5. Finally, the sample was exhaustively dialyzed and concentrated with polyethylene glycol in buffer 3 at 4 °C. The pyridoxal-GluDH derivative was concentrated from 1 to 15 mg/ml. At this point, the modified enzyme was centrifuged at the settings given above. The percentage of active sites tagged at lysine 126 was determined by monitoring the absorbance at 280 and 327 nm. At the latter wavelength, the absorption coefficient for pyridoxal 5'-phosphate is $1.07 \cdot 10^4$ $cm^{-1}M^{-1}$ [22]. Recall from the immobilization section, $\epsilon_{280\,nm}$ is 0.93 ml $mg^{-1}cm^{-1}$ for GluDH. Then, the spin-labeling procedure was implemented.

For the immobilized enzyme, free GluDH modified with pyridoxal 5'-phosphate was concentrated in buffer 1 at 4°C to 5 mg/ml. Immobilization

and spin labeling followed the absorbance measurements at 280 and 327 nm.

Fluorescent illumination of immobilized GluDH distribution

The internal distribution of GluDH in the Sepharose beads was visualized by binding fluorescein isothiocyanate to the immobilized protein, splitting the beads with a microtome and observing the fluorescence microscopically [9,23]. As a control, the barren support matrix was exposed to fluorescein isothiocyanate; the fluorescence of this Sepharose control was negligible.

Results

Immobilization and resulting GluDH distribution

In the past, GluDH was immobilized on CNBr-activated Sepharose for kinetic and medical investigations [6,24]. To our knowledge, the research presented here was the first attempt at examining the immobilized enzyme with ESR spectroscopy. To detect a signal from the ketone probe, this spectroscopy study required higher concentrations of the hexamer within the bead than could be achieved with previous protocols.

The penetration of an enzyme into a porous bead is a function of the immobilizing conditions, structural dimensions of the protein and pore size of the support [23]. At concentrations present during immobilization, GluDH will assume an aggregated state in 0.1 M phosphate buffer, pH 8.0. The resulting rodlike structures have lengths on the order of 100 nm [19]. With an average Sepharose pore size of 300 Å, only a monolayer coverage on the outer surface of the bead is expected. When spin labeled, this GluDH loading would have produced, at best, a very weak spectrum. To increase penetration, the biocatalyst was attached to the support matrix in a 10% dioxane solution. This separated the enzyme into active hexamers [14]. Then, the hexamer, with an overall dimension of approximately 85 × 110 Å [3], was coupled to Sepharose via primary amino groups (Fig. 1.1) [15,25,26].

Like dioxane, GTP and NADH promote dissociation of the GluDH aggregate [3]. Washing GluDH covalently bound to carbodiimide-activated succinamidopropyl-glass beads with 20 μM GTP and 100 μM NADH caused the aggregated, immobilized enzyme to dissociate. This left only hexamers bound to the support [27]. If GTP and NADH were substituted for dioxane

in our immobilization procedure, protein loading on CNBr- or CH-activated Sepharose would not be maximized. Both GTP and NADH contain primary amino groups and, thus, would compete with the enzyme for binding sites on the Sepharose matrix.

The resulting GluDH distribution from the dioxane immobilization was visualized with fluorescein isothiocyanate. Figure 1.2 shows a cleaved surface on the right and, for comparison, the exterior of an intact bead on the left. The photo reveals that GluDH was confined to a spherical shell, penetrating approximately 8 μm into a bead with an average radius of 50 μm.

Deconvolution of experimental ESR spectra into components

In this work, populations of spin labels are classified according to mobility. The motion of the spin label is characterized by line broadening and outer peak separation of the ESR signal. The more mobile the spin label is, the smaller these parameters become [9,17,28]. Two populations of ketone labels are clearly visible in Figures 1.3, 1.4, 1.7 and 1.8. The more mobile component (population A) has an outer peak separation of 33 G; the restricted component (population B), 69 G. The deconvoluted line shapes of these two components are shown in Figures 1.5 and 1.6. The line shape for population B (Fig. 1.6) appears to be contaminated by a relatively small quantity of ketone labels that has a mobility unlike those of the two principal populations. The similarity of the line shape in Figure 1.5 and that of freely tumbling ketone label in a 95% (w/v) glycerol solution at 20°C [17] suggests that the former represents a single population of ketone labels. To determine whether or not these deconvoluted spectra are truly representative of populations A and B, all experimental spectra described in this paper were reconstructed from a linear combination of the

spectra in Figures 1.5 and 1.6. The reconstructed line shapes closely follow the experimental spectra (Fig. 1.8).

Properties of free and immobilized GluDH after standard labeling

Ketone-labeled GluDH was characterized according to its residual activity, the amount of label incorporated into the enzyme, and the percentage of those labels belonging to population A. In the following, the enzyme will be analyzed from these three perspectives.

To calculate the percentage of ketone labels that are in population A, the experimental spectra were divided into two rather than three components. The subpopulation in Figure 1.6 was lumped with population B because there was insufficient information to isolate it. Using this convention, we determined that 10% (Table 1.1) of the ketone labels bound to free GluDH are in population A under standard labeling conditions as compared to 34% (Table 1.2) for the immobilized enzyme. This percentage is unaffected by exposing free GluDH to a buffer containing sodium phosphate rather than Tris while recording the spectrum. For immobilized GluDH, neither separating the hexamer from the support matrix with a six-carbon spacer arm nor varying the protein loading within the support matrix changes the percentage of "A" labels.

Under standard labeling conditions, 83% of the free protomers are spin labeled (Table 1.1). The residual activity is only 17%. Estimates of the percentage of spin-labeled protomers are subject to errors on the order of 10%. For example, a 94% labeling was achieved in a free enzyme sample that was incubated with the ketone label for less time than that required to achieve the 83% labeling. Moreover, Andree and Zantema indicated that 17% residual activity corresponds to approximately 95% of the protomers being labeled [11].

Our activity measurements are reproducible within ± 5%. As will be discussed later, the sum of the percentage of labeled protomers and the percentage of residual activity can be greater than 100% (Tables 1.1 & 1.2). This is not due to experimental error; it indicates that the binding site for population A does not participate in catalysis.

When GluDH is immobilized to CNBr-activated Sepharose 4B, labeling is maximized 48 hr after the $NaBH_4$ reduction (Table 1.2). The extent of labeling changes by only 10% after 5 hr. Within 2%, labeling is complete in a day. In this research, we have assumed that the 48 hr incubation allows all binding sites for the ketone label which remain accessible after immobilization to be labeled. Those sites that are inaccessible have either reacted with the support matrix or become blocked by an adjacent hexamer or by the support. This assumption is reasonable since the molar ratio of the ketone label to total immobilized protomer during the $NaBH_4$ reduction is at least 10 times greater than that required to label 88.5 ± 5.5% of free GluDH (Table 1.1). Moreover, no additional labeling occurs in the immobilized enzyme when the molar ratio of $NaBH_4$ to the ketone label is increased by a factor of 10.

Substrate saturation study of free GluDH

In this study, the active site of GluDH was saturated with 16 mM α-ketoglutarate and 3 mM NADH to inhibit ketone labeling. Experimental conditions were chosen to minimize secondary reactions between substrates and the ketone label which would distort the results from this study. Specifically, α-ketoglutarate was chosen because it does not contain primary amino groups which could have reacted with the ketone label during the $NaBH_4$ reduction. NADH has two primary amino groups per molecule; however, the molar ratio of

NADH to the ketone label was 0.02. With such a low ratio, the NADH amino groups could have reacted with only a negligible fraction of ketone labels. The advantages that NADH provided in this experiment were a tighter substrate binding and greater coverage of the active site. In addition to secondary reactions, substrates could have distorted data if they were to remain in the GluDH sample while its ESR spectrum was recorded. For this reason, substrates were removed from the sample by dialysis after the $NaBH_4$ reduction.

In a phosphate buffer (pH 8.0) containing 16 mM α-ketoglutarate and 3 mM NADH, 99.3% of the enzyme is in a NADH-α-ketoglutarate-GluDH complex [20]. Under these conditions, the extent of labeling is reduced from 94 to 22% (Table 1.1). Examining this reduction in terms of the two populations of ketone labels shows that saturation prevents 51% and 79% of the labels in populations A and B, respectively, from binding to free GluDH. This difference is reflected in the line shape of the ESR signal: population A accounts for 21% of the spectrum from this substrate saturation experiment (Fig. 1.7) as compared to 10% under standard labeling conditions (Fig. 1.3).

Pyridoxal 5'-phosphate study of free and immobilized GluDH

The purpose of this study was to characterize the binding site(s) for the ketone label by the effect that pyridoxal 5'-phosphate had on populations A and B. For free GluDH, the extent of ketone labeling is reduced from 75 to 48% when 39% of the protomers are modified with pyridoxal 5'-phosphate (Table 1.1). The percentage of population A in the ESR spectrum is unaffected by the pyridoxal 5'-phosphate modification. Thus, labels in populations A and B are equally reduced. The above percentages appear to be reliable. Andree's and Zantema's data show that free enzyme samples

with 40% residual activity have 70% of their protomers labeled as compared to our value of 75% [11]. Other experiments that we performed with pyridoxal 5'-phosphate suggest that a 39% labeling in a free enzyme sample retaining 56% of its initial activity is reasonable: free GluDH samples in which 46 and 57% of the protomers are modified with pyridoxal 5'-phosphate have residual activities equal to 45 and 35%, respectively. To the best of our knowledge, no comparative data are available for a GluDH sample containing both pyridoxal 5'-phosphate and the ketone label. In our study, this enzyme sample had a total of 0.87 mole label per mole protomer (0.39 from pyridoxal 5'-phosphate and 0.48 from the ketone label). A residual activity of 21% is quite reasonable for such an extensive labeling.

In the experiments with immobilized GluDH, the enzyme was modified with pyridoxal 5'-phosphate prior to immobilization. (This sequence was required to ensure that the binding site(s) for pyridoxal 5'-phosphate was (were) the same in free and immobilized GluDH.) Ketone labeling followed immobilization. Under these conditions, the extent of ketone labeling is reduced from 98 to 44% by modifying 50% of the protomers with pyridoxal 5'-phosphate. As in the free GluDH experiment, the percentage of population A in spectra of the immobilized enzyme is unaffected by immobilization. Unlike the free enzyme, there are no comparative data for immobilized GluDH. However, the following suggests that our data are reliable. When 50% of the protomers are modified with pyridoxal 5'-phosphate, there is a parallel loss in activity of approximately 50%. Moreover, when ketone labeling is reduced by 55% (0.98 to 0.44 mole ketone label per mole protomer), the activity drops by a comparable 46%.

Discussion

In addition to our own investigation, there have been three studies of free GluDH with the ketone label [11,12,13]. In each study, the overall line shape of the ESR spectrum is different; however, each spectrum is a composite consisting of two components, populations A and B. None of these studies acknowledged the other two. Moreover, only Andree and Zantema indicated that their spectra contain more than one population of ketone labels [11]. Specifically, their ESR signal of the free enzyme is identical to ours in Figure 1.3. According to Andree and Zantema, 5 to 10% of the labels belonged to population A in free GluDH samples that contained from approximately 0.1 to 1.2 mole ketone label per mole protomer.

We were able to reconstruct the spectra in References 11 through 13 from a linear combination of the line shapes in Figures 1.5 and 1.6. In this way, we determined that population A accounts for 4% of Iwatsubo's and co-workers' spectrum of free GluDH in 0.1 M Tris/ 0.5 mM EDTA buffer (pH 7.5) at 25°C [13]. Only 15% of their protomers were labeled. Their labeling protocol was not described. In addition, we found that approximately 26% of the ketone labels belonged to population A in a free GluDH sample prepared by Agadzhanyan et al. [12]. Their spectrum was recorded while GluDH was in a 0.02 M potassium phosphate buffer (pH 7.8). Although labeling conditions for this sample were given [29], the percentage of labeled protomers was not. Our findings in Table 1.1 show that the ESR spectrum is not affected by the buffers used in these two studies. Without a thorough description of the experimental conditions, we are unable to pinpoint which factors changed the percentage of "A" labels in these two studies.

In our own study, the percentage of labels belonging to population A is affected by substrate saturation (Fig. 1.7) and immobilization (Fig. 1.4). The simultaneous existence of two populations of spin labels in our spectra indicates that either the ketone label is binding to two sites per protomer (aspecific labeling) or protomers are structurally heterogeneous when labeling occurs at a single site. In the following paragraphs, the feasibility of aspecific labeling and structural heterogeneity will be discussed. Then, changes in the percentage of "A" labels will be examined from these two perspectives.

With tryptic digestion and amino acid hydrolysis, Agadzhanyan et al. determined that the ketone label binds exclusively to lysine 126 [29]. Since this group did not acknowledge multiple populations of ketone labels in their ESR spectrum of free GluDH, perhaps they overlooked a second binding site for population A which accounts for only 26% of their total ESR signal. Thus, the only conclusion one can make with confidence from this study is that population B binds to lysine 126. This residue is located on the perimeter of the active site and is adjacent to (or at most overlaps) the binding site for α-ketoglutarate [30].

If lysine 126 is the only binding site for the ketone label, then the two populations in Figure 1.3 correspond to two structural conformations in the vicinity of this residue. The subpopulation in Figure 1.6 could represent structural diversity within the two principal conformations. For the purpose of this discussion, these two principal conformations will be referred to as "A" and "B" with the convention that conformation A corresponds to population A. Then, Figure 1.3 represents a free GluDH sample in which 10% of the protomers have adopted conformation A to form a structurally heterogeneous hexamer.

Since all six protomers have identical amino acid sequences, it is doubtful that structural heterogeneity would be intrinsic to the native enzyme. More likely, heterogeneity would be induced in a homogeneous hexamer by substrates as part of an allosteric regulatory mechanism. Indeed, ESR [5] and fluorescence spectra [31] have detected structural change induced by α-ketoglutarate and glutamate. In this regard, spin labeling may mimic substrate binding: the ketone label may induce structural heterogeneity in the GluDH hexamer upon binding to lysine 126 on the perimeter of the active site.

The relationship between residual activity and labeled protomers can be explained equally well with either aspecific labeling or structural heterogeneity. The sum of the percentage of residual activity and the percentage of ketone-labeled protomers can be greater than 100% (Tables 1.1 & 1.2). For example, Andree and Zantema reported that 10% of the initial activity remains when 100% of the protomers are labeled [11]. If labeling is aspecific, then this relationship indicates that lysine 126 (represented by population B) participates in catalysis and that the secondary binding site (represented by population A) does not. If, however, labeling occurs exclusively at lysine 126, then this relationship suggests that residual activity is dependent on the conformation of the protomer. Data in Tables 1.1 and 1.2 would be produced if a ketone-labeled protomer with conformation A was functional and was inactive when the conformation was "B." This suggests that lysine 126 does not participate in catalysis and that ketone labeling eliminates activity through steric hindrance.

Substrate saturation

Saturation of the active site with α-ketoglutarate and NADH increases the percentage of "A" labels from 10 to 21 (Table 1.1). It is unlikely that this

increase is an artifact of a lower labeling and, thus, aggregation. Like pyridoxal 5'-phosphate [21], the ketone label may dissociate aggregated GluDH. Dissociation may increase as more protomers are spin labeled. At protein concentrations used in this study, GluDH was aggregated prior to labeling [19]. After labeling, the substrate saturation sample containing 0.22 mole label per mole protomer could have been more aggregated than its control with 0.94 mole label per mole protomer (Table 1.1). As GluDH aggregates, its protein tumbling frequency decreases. The mobility of a spin label is a function of this protein tumbling as well as the rotational freedom around the bond which fastens the label to the protein [9,28,32]. If the ketone labels represented in Figures 1.3 and 1.7 were dominated by protein tumbling, then the lower labeling in the substrate saturation experiment would have decreased the percentage of labels in population A, the more mobile component. Since this is not the case (Fig. 1.7), the increase in the percentage of "A" labels was caused by the substrates and not the lower labeling. This theoretical argument is supported by Andree's and Zantema's data. Using our standard labeling protocol, they found that free GluDH samples, containing from 0.1 to 1.2 mole label per mole protomer, have ESR spectra in which population A accounts for no more than 10% of the total signal [11].

The increase in the percentage of "A" labels from 10 to 21 (which corresponds to a 51 and 79% reduction of populations A and B, respectively) would be expected in a protomer containing two binding sites for the ketone label. It would also occur in a structurally heterogeneous hexamer containing a single binding site per protomer if the dissociation constants for the two substrates were different for the two structural conformations represented by populations A and B. Dissociation constants for α-ketoglutarate and NADH would be larger

in conformation A than in conformation B. The existence of two sets of dissociation constants seems reasonable in light of other binding studies. For example, NAD has a dissociation constant of 6 μM when glutarate is present and the concentration of NAD is below 20 μM. Above this concentration, the dissociation constant is 40 μM [33].

Immobilization

Sepharose-immobilization increases the percentage of ketone labels in population A from 10 to 34 (Tables 1.1 & 1.2). This could be due to a change in protein tumbling, in binding sites for the ketone label, in binding affinities for these sites and to structural heterogeneity. Each of these factors will be addressed below.

As in the substrate saturation experiment, ESR spectra of immobilized GluDH are unaffected by changes in protein tumbling. If there were a dependence, then the restriction of protein tumbling that accompanies immobilization would lower the percentage of "A" labels. The opposite is observed (Figs. 1.3 & 1.4). Thus, spectra of immobilized GluDH reflect the structure of the spin-labeled region rather than protein tumbling [9,28,32].

Given that spectra of the immobilized enzyme represent surface structure, does the increase in the percentage of ketone labels in population A signify a change in the binding site(s) for the ketone label? For free GluDH, it has been proposed that lysine 126 attracts the ketone label because this residue has an abnormally low pK, 7.8. This low value may be caused by neighboring amino acids that are positively charged [12]. Structural changes induced

by immobilization could, for instance, move the binding site for the ketone label by increasing the distance between the positively charged amino acids and lysine 126.

The purpose of the pyridoxal 5'-phosphate study was to characterize the binding site(s) for the ketone label on free and immobilized GluDH. If the ketone label and pyridoxal 5'-phosphate were binding to different residues, then ketone labeling would be uninhibited by pyridoxal 5'-phosphate. Instead, labeling is reduced by 36 and 55% in free and immobilized GluDH, respectively (Tables 1.1 & 1.2). If only the "A" labels were binding to a different residue, then the percentage of "A" labels in the ESR signal would rise from 10 to 15.5 for the free enzyme and 34 to 51 for the immobilized enzyme. Tables 1.1 and 1.2 show that no change was observed. These results indicate that, first, immobilization has no effect on the binding site(s) for the ketone label and, second, the binding sites for the ketone label and pyridoxal 5'-phosphate are the same.

Piszkiewicz et al. determined that pyridoxal 5'-phosphate binds exclusively to lysine 126 [34]. Their procedure was similar to that used by Agadzhanyan et al. in identifying the binding site for the ketone label. Thus, it is possible that both these groups overlooked a secondary binding site. However, if both groups are correct, then our pyridoxal 5'-phosphate study shows that populations A and B bind to the same residue, lysine 126.

Since the ESR spectrum in Figure 1.4 is not influenced by protein tumbling or a change in binding site(s) for the ketone label, the increase in the percentage of "A" labels from 10 (free GluDH) to 34 (immobilized GluDH) reflects a greater affinity of the ketone label for the secondary site if it exists. Otherwise, it reflects a more structurally heterogeneous hexamer. In either case,

immobilization does not distort the structure of the enzyme. This may represent a fundamental difference between immobilizing a monomer and oligomer. ESR spectra of α-chymotrypsin, a monomer, show that this enzyme is distorted into a more contracted shape during Sepharose-immobilization [9]. Unlike chymotrypsin, GluDH undergoes conformational change [5,31]. Possibly, the hexamer can adopt the conformation which minimizes the strain imposed on it by immobilization. Since chymotrypsin has only one conformation, its structure is distorted to minimize this stress.

If this scenario is correct, the percentage of "A" labels bound to immobilized GluDH should be related to the quaternary structure [3,4] of the enzyme at maximum labeling. This requires that the percentage of "A" labels be equal to a multiple of one-sixth. No relationship is apparent in free GluDH: after standard ketone labeling, no more than 10% of the labels belong to population A in free enzyme samples containing as much as 1.2 mole label per mole protomer (Table 1.1 and Reference 11). For the immobilized enzyme, 34% corresponds to two-sixths. This strongly suggests that immobilization causes two protomers to adopt a conformation different from that of the other four. If labeling is aspecific, then this structural heterogeneity is reflected indirectly in the increased binding of the ketone label to these two protomers at the secondary site. If labeling occurs exclusively at lysine 126, then the heterogeneity is reflected directly in the two structural conformations at this residue.

In this paper, the overall ESR spectrum of GluDH was changed by altering the enzyme's environment during ketone labeling with substrate saturation and immobilization. As factors in the environment which influence the properties of an enzyme become better understood, it may be possible to optimize these

properties for a particular set of processing conditions. To this end, this study suggests ways to selectively modify and induce structural heterogeneity in an oligomer.

Footnote

1 Previous investigators found that 100 mM α-ketoglutarate blocks the ketone probe from binding to the free enzyme [12]. Since we determined that additional labeling occurs after 5 hr with the immobilized enzyme (Table 1.2), α-ketoglutarate was included in the first dialysis to prevent the nitroxide from attaching to free GluDH as NADH diffused out of the sample.

References

1 Engel, P. C. and Dalziel, K. (1969) Biochem. J. 115, 621-631

2 Struck, J., Jr. and Sizer, I. W. (1960) Arch. Biochem. Biophys. 86, 260-266

3 Sund, H., Markau, K. and Koberstein, R. (1975) in Biological Macromolecules, Subunits in Biological Systems, Part C, vol. 7 (Timasheff, S. N. and Fasman, G. D., eds.), pp. 225-287, Marcel Dekker, New York

4 Hucho, F. and Janda, M. (1974) Biochem. Biophys. Res. Commun. 57, 1080-1088

5 Zantema, A., Vogel, H. J. and Robillard, G. T. (1979) Eur. J. Biochem. 96, 453-463

6 Cooper, A. J. L. and Gelbard, A. S. (1981) Anal. Biochem. 111, 42-48

7 Gelbard, A. S., Benua, R. S., Reimam, R. E., McDonald, J. M., Vomero, J. J. and Laughin, J. S. (1980) J. Nucl. Med. 21, 988-991

8 Yoshimoto, T., Takahashi, K., Nishimura, H., Ajima, A., Tamaura, Y. and Inada, Y. (1984) Biotechnol. Lett. 6, 337-340

9 Clark, D. S. and Bailey, J. E. (1983) Biotechnol. Bioeng. 25, 1027-1047

10 Wagner, T. E. and Hsu, C.-J. (1970) Anal. Biochem. 36, 1-5

11 Andree, P. J. and Zantema, A. (1978) Biochemistry 17, 778-783

12 Agadzhanyan, S. A., Pogosyan, A. A. and Karabashyan, L. V. (1982) Mol. Biol. (Moscow) 16, 345-351

13 Iwatsubo, M., Jallon, J. M. and Di Franco, A. (1973) in Dynamic Aspects of Conformational Changes in Biological Macromolecules (Sadron, C., ed.), pp. 431-445, D. Reidel Publishing, Dordrecht-Holland

14 Churchich, J. E. and Wold, F. (1963) Biochemistry 2, 781-786

15 (1983) Affinity Chromatography: Principles and Methods, pp. 12-18 & 24-27, Pharmacia Fine Chemicals, Sweden

16 Frieden, C. (1962) J. Biol. Chem. 237, 2396-2400

17 Jost, P. and Griffith, O. H. (1972) Methods Pharmacol. 2, 223-276

18 Ford, J. R., Lambert, A. H., Cohen, W. and Chambers, R. P. (1972) Biotechnol. Bioeng. Symp. No. 3 267-284

19 Sund, H. and Burchard, W. (1968) Eur. J. Biochem. 6, 202-206

20 Engel, P. C. and Dalziel, K. (1970) Biochem. J. 118, 409-419

21 Anderson, B. M., Anderson, C. D. and Churchich, J. E. (1966) Biochemistry 5, 2893-2900

22 Chen, S.-S. and Engel, P. C. (1975) Biochem. J. 147, 351-358

23 Dennis, K. E., Clark, D. S., Bailey, J. E., Cho, Y. K. and Park, Y. H. (1984) Biotechnol. Bioeng. 26, 892-900

24 Havekes, L., Bückmann, F. and Visser, J. (1974) Biochim. Biophys. Acta 334, 272-286

25 Kohn, J. and Wilchek, M. (1981) Anal. Biochem. 115, 375-382

26 Cuatrecasas, P. and Parikh, I. (1972) Biochemistry 11, 2291-2299

27 Horton, H. R., Swaisgood, H. E. and Mosbach, K. (1974) Biochem. Biophys. Res. Commun. 61, 1118-1124

28 Morrisett, J. D. (1976) in Spin Labeling: Theory and Applications (Berliner, L. J., ed.), pp. 273-338, Academic Press, New York

29 Agadzhanyan, S. A., Arutyunyan, A. A. and Karabashyan, L. V. (1984) Bioorg. Khim. 10, 1171-1176

30 Zantema, A., De Smet, M.-J. and Robillard, G. T. (1979) Eur. J. Biochem. 96, 465-476

31 Bell, E. T., LiMuti, C., Renz, C. L. and Bell, J. E. (1985) Biochem. J. 225, 209-217

32 Morrisett, J. D., Broomfield, C. A. and Hackley, B. E., Jr. (1969) J. Biol. Chem. 244, 5758-5761

33 Dalziel, K. and Egan, R. R. (1972) Biochem. J. 126, 975-984

34 Piszkiewicz, D., Landon, M. and Smith, E. L. (1970) J. Biol. Chem. 245, 2622-2626

Table legends

Table 1.1 Properties of free GluDH labeled under a variety of experimental conditions. Experimental conditions for labeling are as described in Materials and Methods with the following exceptions: A, none; B, spectra were recorded with GluDH in 0.02 M potassium phosphate buffer (pH 7.8); C, spectra were recorded with GluDH in 0.1 M Tris/0.5 mM EDTA buffer (pH 7.5); D (control for E), second incubation of GluDH with the ketone label required 4 hr at 25°C; E, ketone labeling was done in the presence of 16 mM α-ketoglutarate and 3 mM NADH as described in Materials and Methods; F, first and second incubations of GluDH with the ketone label required 1 hr and 2.5 hr at 4°C, respectively; and G, none. The procedure for determining the percentage of "A" labels is given in Materials and Methods. Reference activity is that of free GluDH prior to labeling.

Table 1.2 Properties of immobilized GluDH labeled under a variety of experimental conditions. Experimental conditions for labeling are as described in Materials and Methods with the following exceptions: A, second incubation of GluDH with the ketone label required 5 hr at 25°C followed by 43 hr at 4°C; B, none; C, loading of GluDH varied from 2.8 to 17 mg labeled protomer/g CNBr-activated Sepharose and from 4.9 to 10 mg labeled protomer/g CH-activated Sepharose; D, second incubation of GluDH with the ketone label required 5 hr at 25°C; and E, none. The procedure for determining the percentage of "A" labels is given in Materials and Methods. Reference activity is that of the immobilized GluDH sample in B prior to labeling.

Table 1.1

Label	Experimental Conditions	% Labels in Population A	% Protomers Labeled	% Residual Activity
KL[w]	A, B, C	10	83	17[y]
KL	D	10	94	z
KL	E	21	22	z
KL	F	10	75	40
Pyr5P[x]	G	—	39	56
Pyr5P, KL	F, G	10	39 (Pyr5P), 48 (KL)	21

[w] Ketone label.

[x] Pyridoxal 5'-phosphate.

[y] Residual activity corresponds to experimental condition A only.

[z] Not determined.

Table 1.2

Label	Experimental Conditions	% Labels in Population A	% Maximum Labeling	% Residual Activity
KL[x]	A	34	100	36
KL	B, C	34	98	37[z]
KL	D	34	90	33
Pyr5P[y]	E	—	50	52
Pyr5P, KL	B, E	34	50 (Pyr5P), 44 (KL)	20

[x] Ketone label.

[y] Pyridoxal 5'-phosphate.

[z] Residual activity corresponds to experimental condition B only.

Figure legends

Fig. 1.1 Immobilization of an enzyme via a primary amino group to CNBr-activated and CH-activated Sepharose 4B.

Fig. 1.2 Distribution of GluDH within a Sepharose support. The microphotogragh (400×) shows a CNBr-activated Sepharose bead containing GluDH labeled with fluorescein isothiocyanate before (left) and after (right) being split by a microtome.

Fig. 1.3 ESR spectrum of ketone-labeled, free GluDH. The formula of the ketone probe is displayed in the upper right-hand corner.

Fig. 1.4 ESR spectrum of ketone-labeled, immobilized GluDH. The enzyme was covalently coupled to CNBr-activated Sepharose 4B.

Fig. 1.5 Deconvoluted spectrum of population A. This line shape was obtained by subtracting the ESR spectrum in Figure 1.3 (multiplied by an adjustable weighting factor) from that in Figure 1.4 and by smoothing the resulting spectrum.

Fig. 1.6 Deconvoluted spectrum of population B. The spectrum in Figure 1.5 was subtracted from that in Figure 1.3 to obtain this line shape. Arrows point to the portions of the line shape which denote a subpopulation.

Fig. 1.7 Spectrum produced from ketone labeling free GluDH in the presence of 16 mM α-ketoglutarate and 3 mM NADH.

Fig. 1.8 Reconstructed spectrum of Figure 1.7 from the deconvoluted line shapes in Figures 1.5 and 1.6 superimposed on the original, experimental spectrum.

Figure 1.1

1) *CNBr-Activated Sepharose 4B*

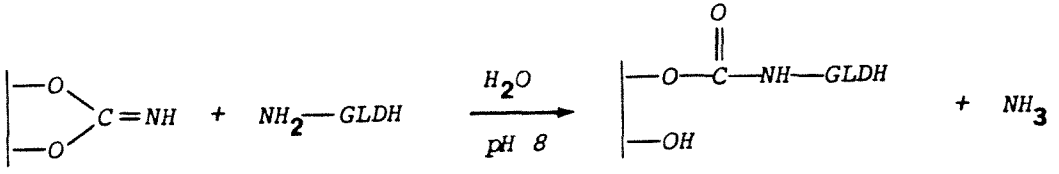

bead

primary amino group

2) *CH-Activated Sepharose 4B*

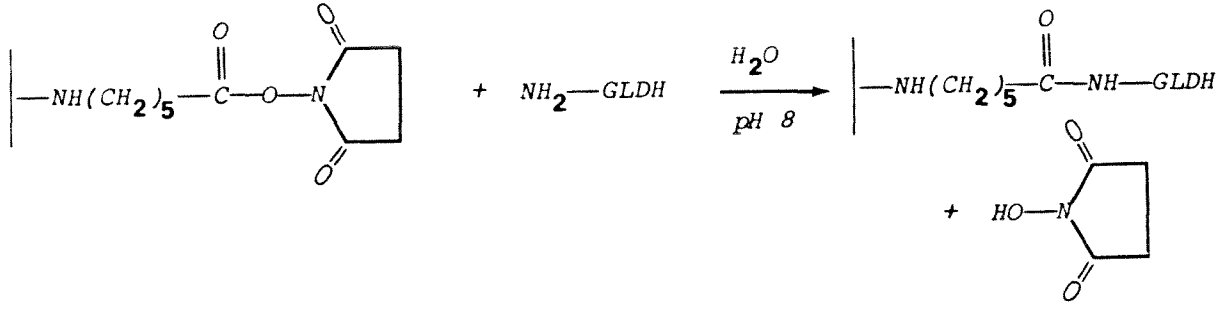

Figure 1.2

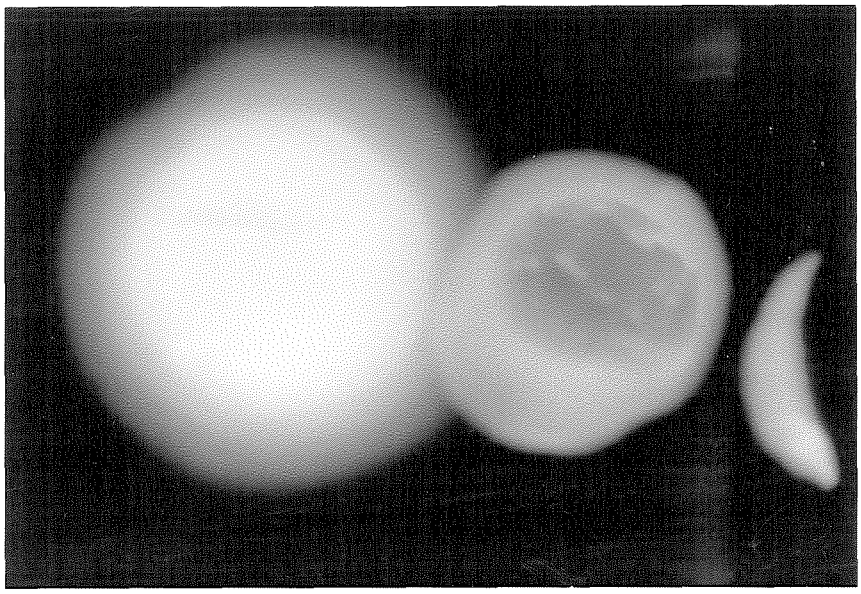

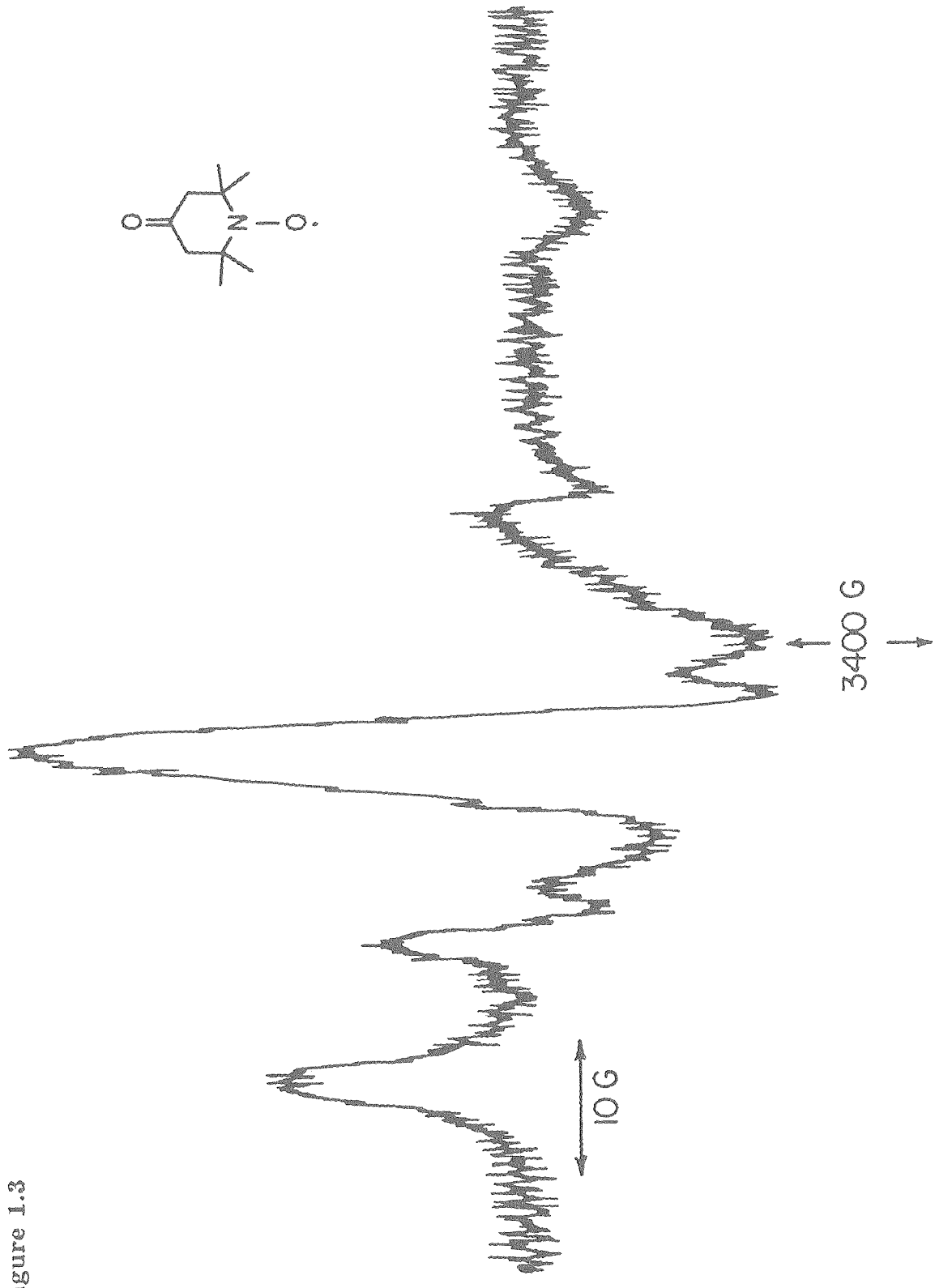

Figure 1.3

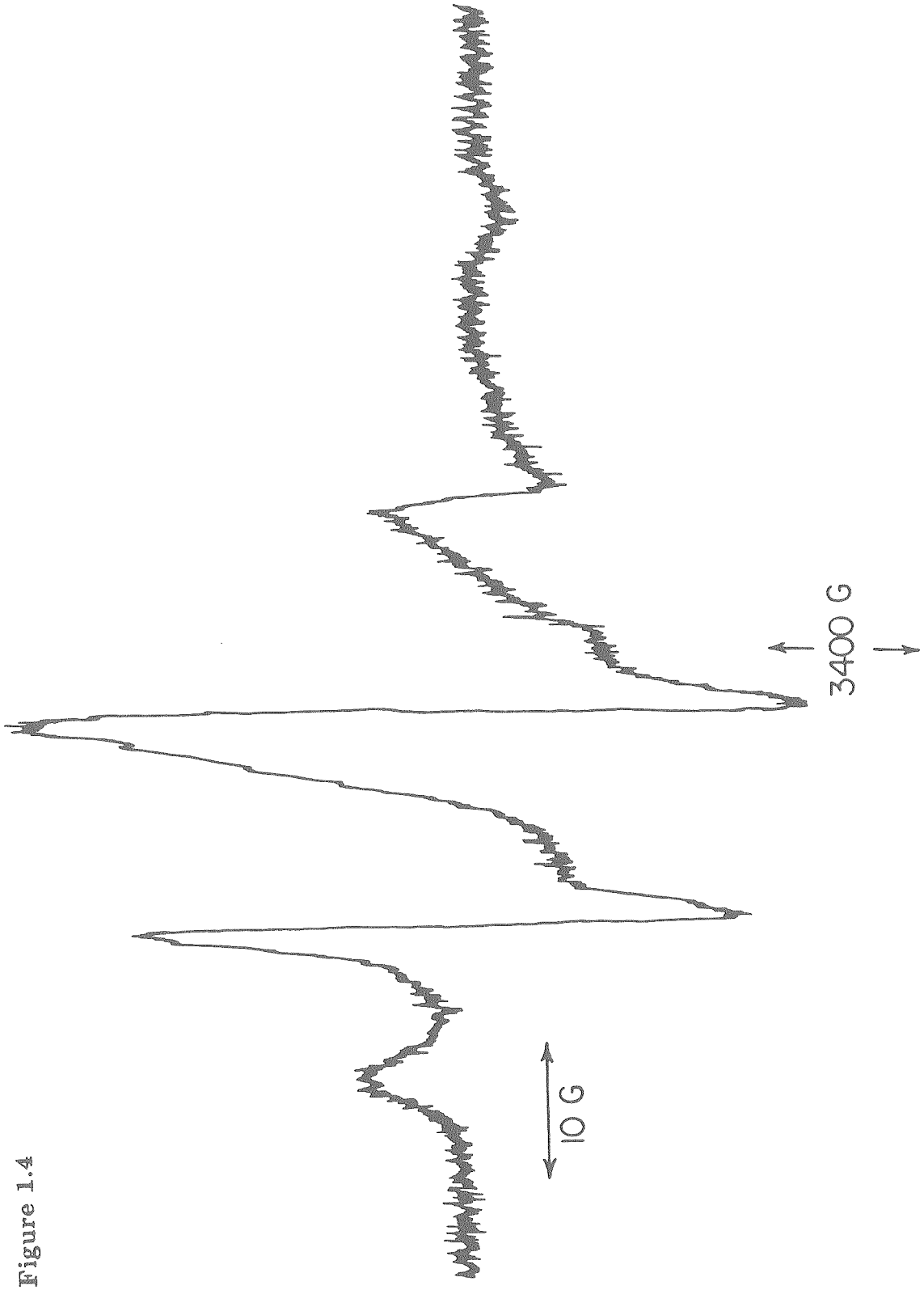

Figure 1.4

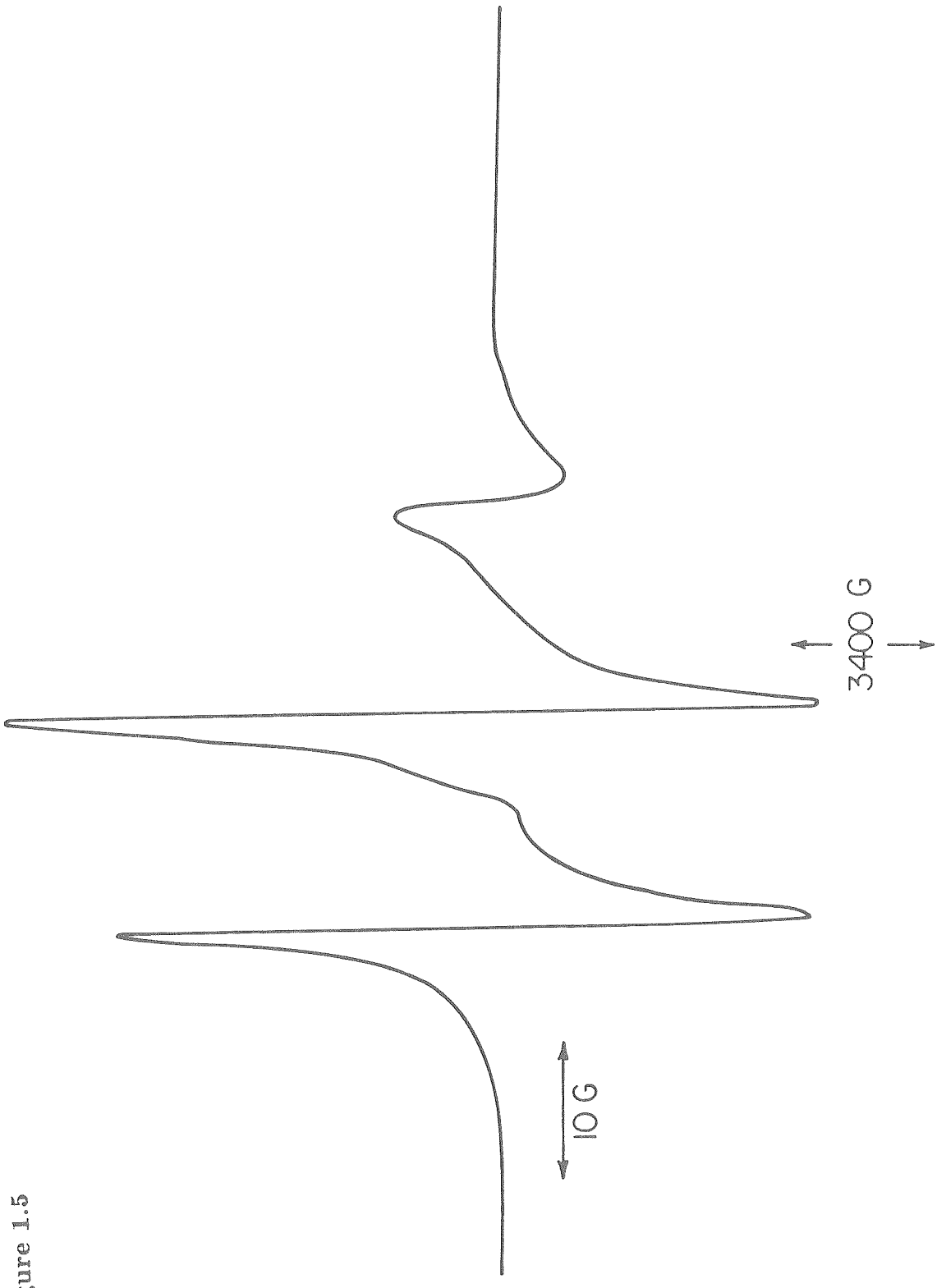

Figure 1.5

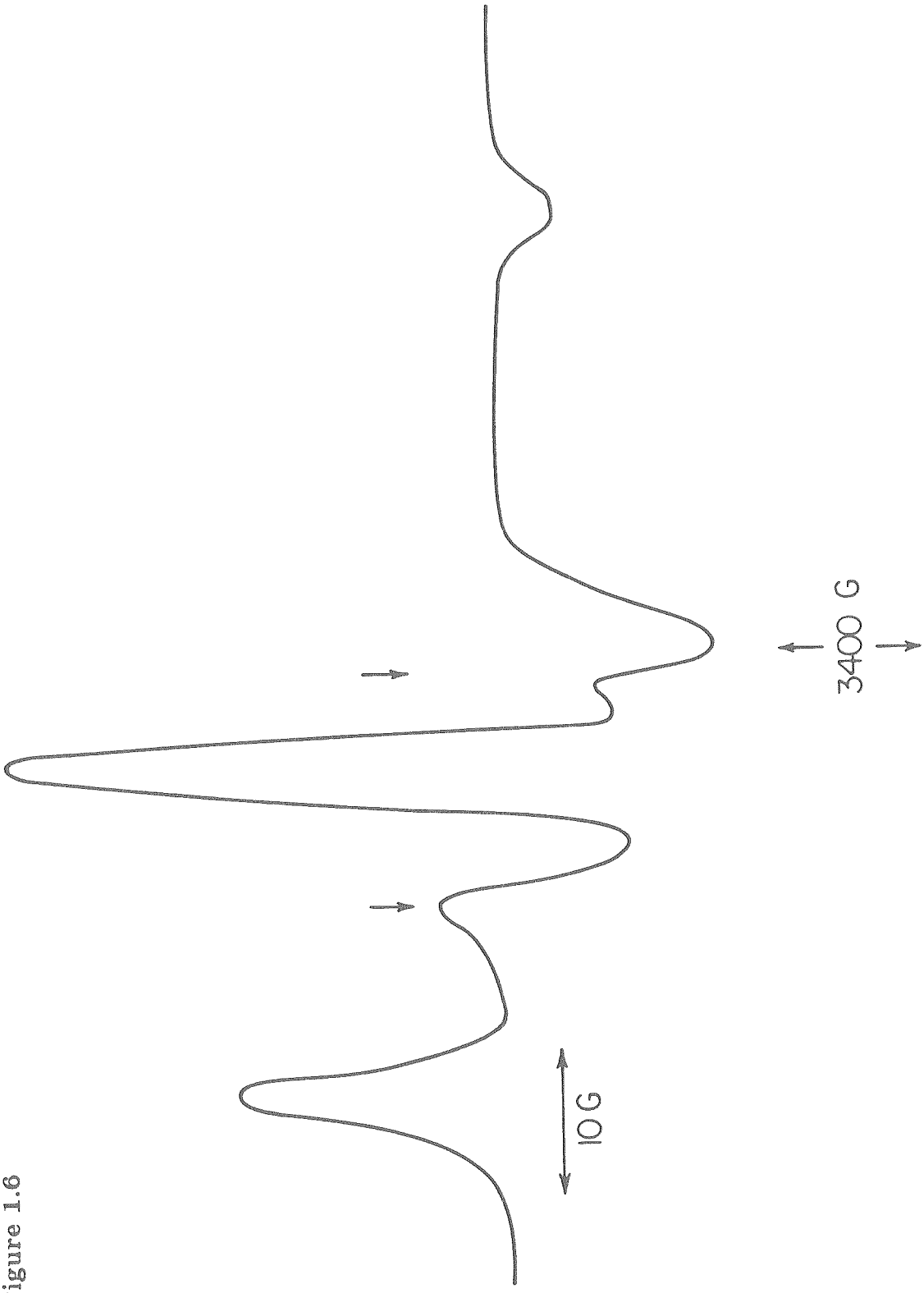

Figure 1.6

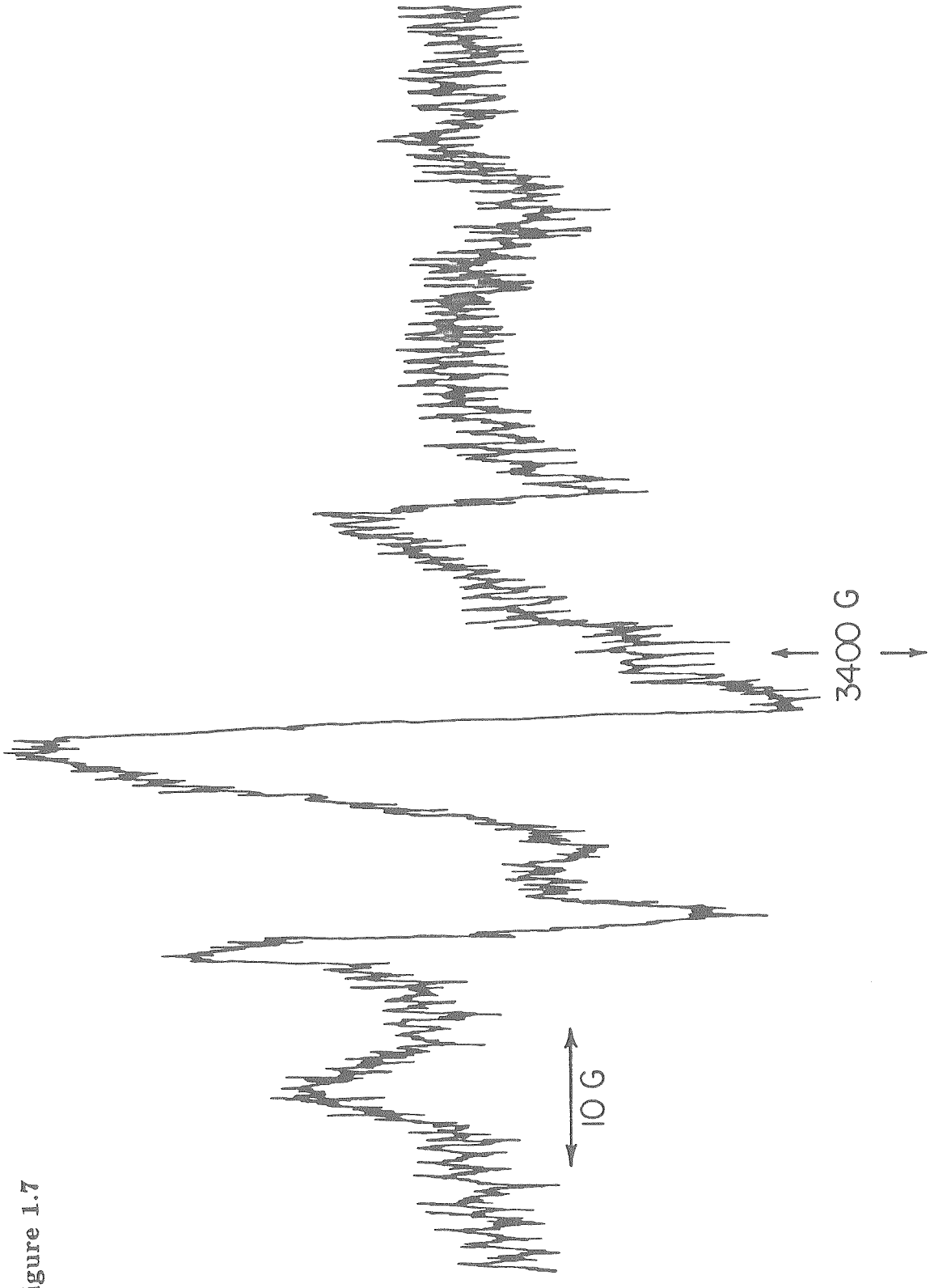

Figure 1.7

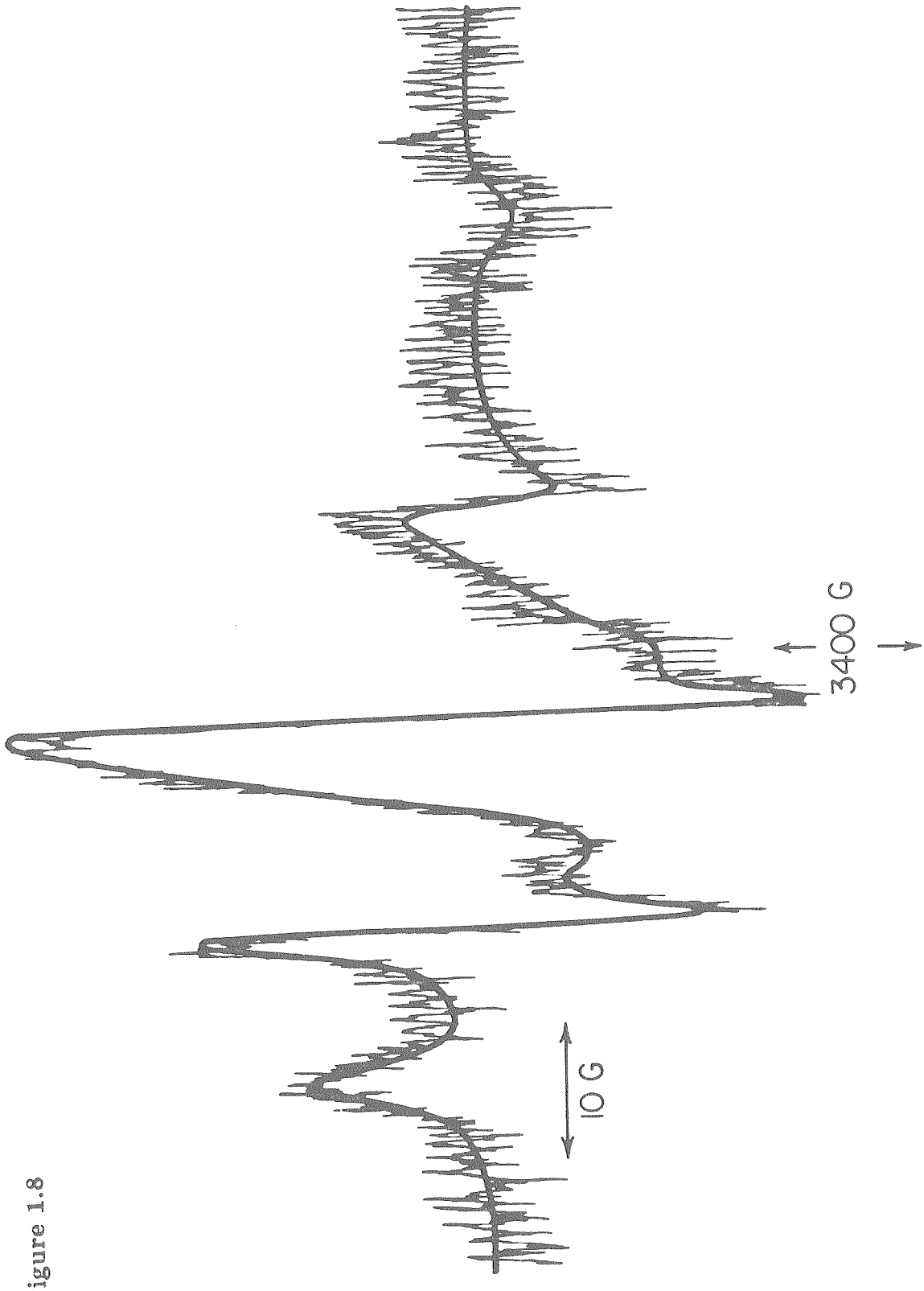

Figure 1.8

CHAPTER 2

Effects of Immobilization on Conformational Change in the Vicinity of Cysteine 319 of Glutamate Dehydrogenase: An ESR Spectroscopy Study

Introduction

This chapter contains the second half of a two part study of GluDH structure with ESR spectroscopy. In Chapter 1, factors in the environment which affect the ESR spectrum of ketone-labeled GluDH were analyzed. One of these factors was immobilization. The research presented in this chapter focuses on the effects of immobilization on conformational change. A byproduct of this study is some additional information on structural heterogeneity.

ESR [1], fluorescence [2] and circular-dichroism spectroscopy studies [3] have shown that GluDH undergoes conformational change which is induced by the binding of ADP, GTP, NAD(P), amino acid substrates and their analogues to the enzyme. In one such study, Zantema et al. monitored conformational change in free GluDH with 4-((4-(chloromercurio)benzoyl)amino)-2,2,6,6-tetramethyl-1-piperidinyloxy (ClHgBz-TEMPO) [1]. This mercuric spin label covalently binds to the free sulfhydryl group on cysteine 319. This amino acid is located in one of two six-stranded parallel β sheets, called domain 3 [4]. Analogous structures in other NAD(P)-binding enzymes suggest that these two regions are NAD(P)-binding sites. For example, mutation studies with *Neurospora crassa* GluDH in which phenylalanine replaced serine 336 in domain 3 suggest that this domain is involved in NAD(P) binding at the active site [5].

In this work, the individual GluDH hexamers were covalently coupled via primary amino groups to CNBr-activated Sepharose 4B (Chapter 1) in order to modify conformational change. The effects of immobilization on this structural property were investigated with ClHgBz-TEMPO and are described below.

Materials and methods

This research required bovine liver GluDH suspended in a 50% glycerol solution (Boehringer Mannheim), custom synthesized ClHgBz-TEMPO according to the procedure in Reference 1 (Molecular Probes), and a total protein assay kit (Sigma, catalog no. 690-A). All other required chemicals and equipment have been mentioned in Chapter 1.

Prior to spin labeling, the concentration of free GluDH was determined spectrophotometrically at 280 nm and 25°C with an absorption coefficient of 0.93 $ml \cdot cm^{-1} \cdot mg^{-1}$ [1]. *As in Chapter 1, one mole enzyme is defined to be one mole protomer.*

Experiments with ClHgBz-TEMPO involved concentrating the initial GluDH solution containing 50% glycerol from 7 to 15 mg/ml at 4°C with 0.1 M sodium phosphate buffer (pH 7.4) containing 12.5% (w/v) polyethylene glycol as described in Chapter 1. Dialysis against 0.1 M sodium phosphate buffer (pH 7.4) at 4°C and centrifugation at 30 000 × g for 20 min at 5°C followed. Zantema's and co-workers' procedure [1] was used to spin label the clarified GluDH solution with ClHgBz-TEMPO. Spectra of GluDH were recorded under the same conditions and analyzed in the same manner as the spectra displayed in Chapter 1. Degassing was not required.

Spectrum Ib (Fig. 2.1) was obtained by dialyzing spin-labeled free GluDH at 4°C against 87 mM sodium phosphate buffer (pH 8.0) and centrifuging as before. Then, 12 ml of 4.3 mg/ml enzyme was coupled to 600 mg CNBr-activated Sepharose 4B and stored according to the protocol in Chapter 1. (One gram beads equals 3.5 ml gel.) One hour prior to recording the ESR spectrum,

100 mg beads in 87 mM sodium phosphate buffer (pH 8.0) was rinsed in 0.1 M sodium phosphate buffer (pH 7.4), filtered until damp, and mixed with 3 ml of the solutions given in the figure legend.

Note that spin labeling preceded immobilization to ensure that cysteine 319 was modified by ClHgBz-TEMPO.

The fraction of protomers labeled at cysteine 319 with ClHgBz-TEMPO is equal to the concentration of spin labels in the free GluDH sample (obtained from the second integral of the ESR spectrum) divided by the total protomer concentration in that sample (determined from Sigma protein assays). Dividing the concentration of spin labels in the immobilized GluDH sample by the fraction of labeled free protomers gives the total concentration of immobilized protomers. Implicit in this calculation is the assumption that spin labeling does not alter the immobilization efficiency of GluDH.

Results and discussion

By labeling the free enzyme with ClHgBz-TEMPO, Zantema et al. detected three GluDH conformations and induced conformational change in the enzyme with substrates and cofactors [1]. Such experiments have been repeated in this study to provide a basis for comparison with the immobilized GluDH spectra. The three GluDH conformations correspond to ESR spectra Ia, II, and III in Figure 2.1. In the absence of substrates and cofactors, free GluDH spin labeled with the mercuric probe is characterized by spectrum Ia. The addition of saturating concentrations of α-ketoglutarate and NAD(P)H, or glutamate and NAD(P)H causes the line shape to become more immobile (spectrum II). In the presence of saturating concentrations of GTP and NAD(P)H, the spin-labeled, free enzyme generates spectrum III which is the least mobile of the three ESR signals.

A comparison of spectra Ia and Ib shows that the ESR signal from ClHgBz-TEMPO-GluDH is only slightly affected by immobilization. The low field peak in spectrum Ib reveals two distinct populations containing approximately equal concentrations of the mercuric label. Spectral changes caused by immobilization reflect changes in structure rather than in protein tumbling (Chapter 1). Under these conditions, the two populations in spectrum Ib represent either a structurally heterogeneous hexamer or two binding sites for ClHgBz-TEMPO per protomer. If the latter interpretation were correct, then these sites would have approximately equal affinities for ClHgBz-TEMPO. Such aspecific labeling would be easily detected in peptide maps used to identify the binding site for ClHgBz-TEMPO [6]. Since only a single binding site, cysteine 319, was found,

the two populations most likely reflect structural heterogeneity. Because spectra Ia and Ib are so similar, this heterogeneity may be present in free GluDH and be enhanced by immobilization. This enhancement was also observed in ESR spectra of ketone-labeled GluDH (Chapter 1).

Immobilizing GluDH on CNBr-activated Sepharose profoundly affected conformational response to substrate and/or effector binding. When immobilized GluDH was exposed to 46 mM (2370) GTP and 4.0 mM (200) NADPH, no change in the ESR signal was detected. Here and in the remainder of this paper, the numbers in parentheses are the molar ratios of the added biochemical to total protomer. These ratios exceed those required to generate spectrum III by a factor of 170 for GTP and 100 for NADPH. A transition from one spectral type to another would be prevented if GluDH were only partially saturated with cofactors. Because of the large molar excess of GTP and NADPH, this scenario is unlikely. Probably, Sepharose immobilization has strongly restricted, if not eliminated, conformational change associated with the transition from spectrum Ia to spectrum III.

Experiments with the GluDH-Sepharose sample and α-ketoglutarate demonstrate that some conformational response to substrate binding remains after immobilization. Adding 100 mM (5150) α-ketoglutarate to the immobilized enzyme caused spectrum Ib to rapidly decay to zero within 5 min at 25°C. Adding as much as 4.0 mM (200) NADPH could not stabilize the signal. When the free enzyme was exposed to 50 mM (150) α-ketoglutarate, it underwent a conformational change represented by a spectrum that was approximately 75% type Ia and 25% type II. Moreover, this ESR signal was stable. It is unlikely that the large molar excess of α-ketoglutarate to total protomer caused the signal decay

in the immobilized GluDH experiments since the two carboxyl groups on this substrate have pK's equal to 4.44 and 1.85 [7] and, thus, are deprotonated at pH 7.4. Probably, reduction of the mercuric label caused this decay. Immobilization may have modified α-ketoglutarate-induced conformational change so that one of the protomer's residues moved to a position where it reduced the spin label. Reductions of spin labels by enzymes have been previously reported [8].

Together, kinetic and spectroscopic studies of GluDH suggest that conformational change induced by NAD(P) and glutamate activates the deamination reaction between these two substrates [2]. In this work, we have successfully modified conformational change in GluDH with Sepharose-immobilization and characterized this modification with ESR spectroscopy. In Chapter 3, these results will be combined with kinetic data from Sepharose-immobilized GluDH to provide insight into the relationship between activation and conformational change. This methodology of studying structure-function relationships may be applicable to other enzymes containing the NAD(P)-binding domain to which ClHgBz-TEMPO was attached: horse liver alcohol dehydrogenase, lobster muscle glyceraldehyde 3-phosphate dehydrogenase, dog-fish M_4 lactate dehydrogenase and *Neurospora* NADP-specific GluDH [4].

References

1 Zantema, A., Vogel, H. J. and Robillard, G. T. (1979) Eur. J. Biochem. 96, 453-463

2 Bell, E. T., LiMuti, C., Renz, C. L. and Bell, J. E. (1985) Biochem. J. 225, 209-217

3 Chen, S.-S., Engel, P. C. and Bayley, P. M. (1977) Biochem. J. 163, 297-302

4 Wootton, J. C. (1974) Nature 252, 542-546

5 Brett, M., Chambers, G. K., Holder, A. A., Fincham, J. R. S. and Wootton, J. C. (1976) J. Mol. Biol. 106, 1-22

6 Cosson, M. P., Gros, C. and Talbot, J. C. (1976) Biochem. Biophys. Res. Commun. 72, 1304-1310

7 Martell, A. E. and Smith, R. M. (1977) Critical Stability Constants, Other Organic Ligands, vol. 3, p. 132, Plenum Press, New York

8 Morrisett, J. D. (1976) in Spin Labeling: Theory and Applications (Berliner, L. J., ed.), pp. 296, 297 & 328, Academic Press, New York

Figure legend

Fig. 2.1 ESR spectra of ClHgBz-TEMPO bound to 326 μM free GluDH (Ia, II & III) and immobilized GluDH (19.4 μmole GluDH/liter CNBr-activated Sepharose gel; Ib) in 0.1 M sodium phosphate buffer (pH 7.4) at 25°C. All samples contain 0.6 mole label/mole protomer. Spectra were recorded under the following conditions: Ia, no additions; Ib, no additions or 46 mM GTP and 4.0 mM NADPH; II, 50 mM α-ketoglutarate and 424 μM NADPH; and III, 4.6 mM GTP and 652 μM NADPH. Spectrum Ib is the average of four 16-min scans. Other spectra were not averaged. Arrows point to different populations of spin labels which contribute to spectrum Ib. The formula for ClHgBz-TEMPO is given in the upper right-hand corner.

Figure 2.1

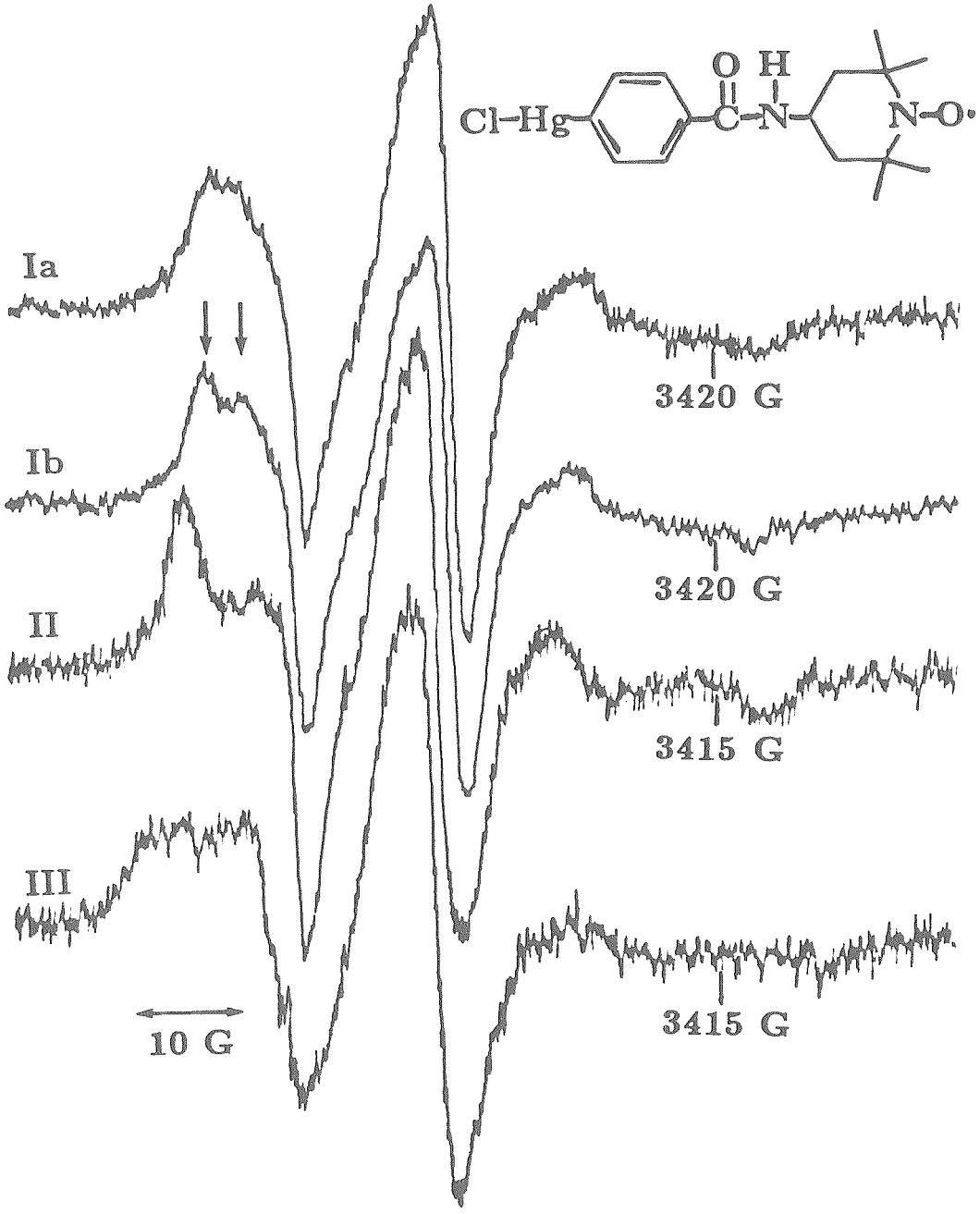

CHAPTER 3

An Application of Enzyme Immobilization for a Kinetic Investigation of NAD and Glutamate Activation Patterns in Glutamate Dehydrogenase

Introduction

In the presence of GluDH, L-glutamate reacts with NAD(P) to produce α-ketoglutarate, NAD(P)H, ammonia and a hydrogen ion. This deamination reaction is reversible and is regulated by substrates, NAD(P), ADP and GTP [1]. This chapter examines the deviation from Michaelis-Menten behavior towards higher activity that is evident from kinetic studies of the deamination reaction. This phenomenon is referred to as substrate activation in this work.

Structural heterogeneity, conformational change and a second, non-catalytic NAD binding site have been cited in the literature as potential sources for substrate activation of free GluDH [2,3]. Much research has been done concerning these three factors. First, data in Chapter 1 suggest that the free enzyme may be structurally heterogeneous. Specifically, the protomer may have primarily two conformations in the vicinity of lysine 126. The reader may recall from Chapter 2 that fluorescence [2], circular-dichroism [4] and ESR spectra [5] have detected conformational change in free GluDH which is induced by the binding of cofactors, substrates or their analogues to the biocatalyst. Apparently to generate this structural response, the glutamate analogue must contain an α-position substituent, be an L-isomer if chiral [2], and have two carboxyl groups separated by the same distance as in glutamate [4]. Compounds which fail to satisfy these requirements, such as norvaline, are unable to induce NAD activation [6]. Wootton reported the existence of two six-stranded parallel β sheet structures in free GluDH which are analogous to NAD(P) binding domains in other enzymes [7].

In this kinetic study, GluDH was covalently bound via primary amino groups to a Sepharose support in order to alter its substrate activation pattern. These

modified activation properties will be analyzed in terms of structural changes that have been induced by immobilization. In this way, the relationship between structure and substrate activation of the free enzyme can be elucidated. Others have also explored GluDH regulation using immobilization. By covalently coupling the biocatalyst to a support, the effects that ADP and GTP have on GluDH activity were investigated in the absence of hexamer association and dissociation that accompanies the binding of these biochemicals to the free enzyme [8]. In addition to examining the regulatory properties of ADP and GTP, Havekes et al. studied NAD and glutamate activation of GluDH immobilized to CNBr-activated Sepharose 4B [9]. Their general theme of comparing the behavior of the free and immobilized biocatalyst is continued in this work which elaborates on Havekes' and co-workers' initial kinetic study by considering the relationship between GluDH structure and catalytic function. To this end, the kinetic results from this investigation were analyzed in terms of previous ESR studies of free and immobilized GluDH structure presented in Chapters 1 and 2.

Materials and methods

Chemicals and equipment

Bovine liver GluDH suspended in a 50% glycerol solution was purchased from Boehringer Mannheim Biochemicals. For other required chemicals and equipment, see Chapter 1.

Preparation and characterization of the GluDH-Sepharose conjugate

The individual GluDH hexamers were covalently bound to either CNBr- or CH-activated Sepharose 4B according to the procedure described in Chapter 1. This produced 500 mg of beads impregnated with protein. Immediately following this step, a 150 mg sample of the immobilized enzyme was assayed for the number of functional protomers that it contained using the ketone-labeling and spectral analysis protocols given in Chapter 1. The remaining 350 mg of beads were reacted with 50 mM glutamate in order to deactivate any residual carboxyl groups on the Sepharose matrix. This prevented artifacts in kinetic assays that could have resulted if glutamate or NAD reacted with the active carboxyl groups. (If only the relative activity is measured at fixed concentrations of both substrates, as was the case in Chapter 1, then this deactivation step is not required.) The 350 mg sample of beads was mixed with 10 ml of 87 mM sodium phosphate buffer (pH 8.0) containing 50 mM glutamate in a 20 ml scintillation vial rotating end-over-end at 13 rpm for one hour at 25°C. This was followed with a one liter wash of 87 mM sodium phosphate buffer (pH 8.0) at 4°C. (Usually 50 mM Tris buffer (pH 8.0) is used to deactivate the carboxyl groups on Sepharose [10]; however, GluDH is unstable in 0.1 M Tris-acetate buffer (pH 8.0) [6]. Glutamate was chosen to replace Tris since it has a primary amino group and, as noted in the stability section of the "Results",

does not deactivate immobilized GluDH. Like glutamate, NAD has these features. Yet, glutamate is the smaller of the two molecules and, as such, could have attached to carboxyl groups that were inaccessible to NAD due to steric hindrance.) After the wash, the GluDH-Sepharose preparation was stored in 87 mM sodium phosphate buffer (pH 8.0) at 4°C and a concentration of 7 to 14 (mg beads)/ml.

Kinetics

The protocol to measure the initial steady state velocities of both free and immobilized GluDH is given in Chapter 1. The reactor system for the immobilized enzyme assays was designed by Ford et al. [11]. As is discussed in the "Comments," activity measurements from this system were free of external and internal transport effects. All other experimental conditions employed here correspond to those of Engel and Dalziel for free GluDH [6], and Havekes et al. [9] for the immobilized enzyme. Kinetic parameters were calculated according to the following convention: *a mole of GluDH is defined as a mole of functional protomers* (see "Comments"). Here, we have assumed that all of the protomers in the free GluDH hexamer are functional.

Because GluDH coupled to CH-activated Sepharose lost 6% of its activity after being stored for two days in 87 mM sodium phosphate buffer (pH 8.0) at 4°C, kinetic assays were performed within a day of completing the immobilized enzyme preparation. Even though the enzyme attached to CNBr-activated Sepharose retained 100% of its activity when stored for a week at 4°C in this phosphate buffer, the timing of the experiments with both support types was the same for consistency.

Comments on interpretation of experimental data

Active site titration

When an enzyme is immobilized, some of its active sites may become blocked by the support, while others become structurally distorted. This is expected to result in a heterogeneous population of functional and inactive biocatalysts within the support matrix [12]. Specific kinetic parameters based only on the total amount of enzyme immobilized reflect a combination of inactivation phenomena and catalytic properties of the active enzyme. However, if these parameters are based only on the amount of functional immobilized enzyme, then they provide a consistent basis for comparing the catalytic function of different catalysts. For this reason, all kinetic constants presented here characterize only functional protomers.

The number of functional protomers in a Sepharose sample was determined by reacting the immobilized enzyme with 2,2,6,6-tetramethyl-4-oxopiperidine-1-oxyl, a nitroxide spin label (Chapter 1). During this reaction, all binding sites for the spin label that remained accessible after immobilization were labeled. The total amount of spin label which had been incorporated into the GluDH-Sepharose sample was determined by comparing the double integral of its ESR spectrum to that from a 925 μM aqueous spin label solution. For this research, we have assumed that the spin label binds exclusively to lysine 126 which is located on the perimeter of the active site [13] and have classified a spin-labeled active site as functional.

There is a possibility that 34% of the spin labels bind to a residue other than lysine 126 (Chapter 1). Further research is needed to determine if this is the case. A secondary binding site would overestimate the number of functional

protomers. To account for this, the GluDH concentrations and apparent rate constants in Tables 3.1 and 3.3 would need to be multiplied by a factor of 0.66 and 1.5, respectively. Dissociation constants would be the same. Since the reported rate constants for some of the GluDH-Sepharose samples are higher than that of the free enzyme by approximately a factor of 2 (Table 3.1), the adjusted rate constants would be even greater. Thus, the conclusion of activity enhancement by immobilization is valid whether or not the number of functional protomers has been overestimated.

Classifying a spin-labeled active site as functional assumes, first, that NAD and glutamate can bind to an active site which is accessible to the nitroxide and, second, that the immobilized enzyme can catalyze the reaction between these substrates once they are bound to the active site. The latter assumption is reasonable since ESR spectroscopy studies revealed that GluDH is not structurally distorted during Sepharose-immobilization (Chapter 1). It is also likely that an active site is equally accessible to the label and glutamate since both chemicals have similar dimensions and their binding sites are adjacent, if not overlapping [13]. Since NAD is a larger molecule than the nitroxide and its adenine ring binds 1.3 nm away from this spin label on the GluDH surface [13], it is possible that this cofactor could be excluded from some of the active sites that bind the nitroxide. If this were the case, active site titration with the spin label would overestimate the number of functional protomers. As before, dissociation constants would be unaffected by this overestimate, and catalytic rate constants would be even larger than those reported in this paper.

External and internal transport effects

Mass transport of substrate influences the apparent catalytic activity of an immobilized enzyme when the catalyzed reaction proceeds faster than the transport process. In our immobilized GluDH system, the substrate experienced primarily two type of mass transport processes: external transport from the bulk fluid to the surface of the Sepharose bead and internal transport (diffusion) within the porous bead. For unambiguous interpretation of reaction kinetic parameters, it is necessary to determine if our immobilized enzyme system was influenced by these two mass transport processes.

The effect of external transport on v, the reaction rate within the Sepharose bead, is described by $\eta_{S,\,e}$, the external effectiveness factor for substrate, S.

$$\eta_{S,\,e} \equiv \frac{v}{v_o} \begin{cases} = 1, & \text{external transport effects are negligible;} \\ < 1, & \text{activity is affected by external transport.} \end{cases} \tag{3.1}$$

In this equation, v_o is the reaction rate that would occur if the exterior surface of the Sepharose bead were exposed to the substrate concentration in the bulk fluid, $[S]_o$ [14]. Cassiere and Carberry determined that in an isothermal system $\eta_{S,\,e}$ is unity when

$$\eta_{S,\,e}\, Da_{S,\,o} < 0.01 \tag{3.2}$$

for reactions of order -1 to 2. $Da_{S,\,o}$, the observable Damköhler number for S, is dimensionless.

$$\eta_{S,\,e}\, Da_{S,\,o} \equiv \frac{v_o}{[S]_o\, k_S\, a}. \tag{3.3}$$

Here, k_S is the mass transfer coefficient for S, and a is the ratio of the external surface area of the Sepharose bead to its volume [14].

Expressions for k_S are dependent on the reactor configuration. The immobilized GluDH reactor is an isothermal packed bed. Under these conditions,

$$k_S \equiv 1.09 \left(\frac{G}{\epsilon_B \rho} \right) (N_{Re} N_{Sc,S})^{-2/3} \tag{3.4}$$

for $1.6 \cdot 10^{-3} < N_{Re} < 5.5 \cdot 10^{1}$. In this equation, G is the mass velocity based on the total cross-sectional area of the reactor; ρ, the fluid density; and ϵ_B, the bed porosity. This porosity is defined as the ratio of the void volume between the Sepharose beads to the total bed volume [15]. The dimensionless groups, N_{Re} and $N_{Sc,S}$, are the Reynolds number and Schmidt number for S, respectively.

$$N_{Re} \equiv \frac{2RG}{\mu}. \tag{3.5}$$

$$N_{Sc,S} \equiv \frac{\mu}{\rho D_S}. \tag{3.6}$$

Here, R is the average radius of a Sepharose bead; μ, the fluid viscosity; and D_S, the diffusion coefficient for S [15].

Our immobilized GluDH reactor was operated at a Reynolds number equal to 0.464. This calculation was based on a R of 50 μm and G of 0.413 g/cm^2 per sec. The mass flow rate was derived from a volumetric flow rate of 33 ml/min, reactor diameter of 13 mm and ρ of 0.997 g/ml, the density of water at 25°C [16]. Like ρ, μ was assumed to be equal to that of water at 25°C, $0.890 \cdot 10^{-2}$ g/cm per sec [16].

The only additional factor required to calculate the Schmidt number is the diffusion coefficient (Equation 3.6). With D_{NAD} equal to $3.3 \cdot 10^{-6}$ cm^2/sec [17],

N_{Sc} is $2.70 \cdot 10^3$ for NAD. A diffusion coefficient, D_{Glu} , equal to $7.4 \cdot 10^{-6}$cm^2/sec was estimated based on a glutamate molar volume, V, of 95.7 ml/mole [16] with Longsworth's relationship for amino acids and peptides in an aqueous solution [18].

$$D_S(cm^2/sec) \cdot 10^6 = \frac{24.182}{[V^{1/3}(ml/mole) - 1.280]} \tag{3.7}$$

The corresponding Schmidt number for glutamate is $1.2 \cdot 10^3$.

To determine k_S (and thus, $\eta_{S,e} Da_{S,o}$), it was assumed that the geometric form of the packed beads was orthorhombic. This packing has an ϵ_B of 0.395 [19]. With this porosity, k_{NAD} equals $9.83 \cdot 10^{-3}$ cm/sec (Equation 3.4). Likewise, k_{Glu} equals $1.69 \cdot 10^{-2}$ cm/sec. Given k_S, values for a, v_o and $[S]_o$ were needed to calculate $\eta_{S,e} Da_{S,o}$. The Sepharose beads have an a value equal to 600 cm^{-1}. Values for v_o and $[S]_o$ are reported in this paper. For all the data plotted in Figures 3.1 through 3.6, $\eta_{S,e} Da_{S,o}$ never exceeded $4 \cdot 10^{-5}$ for NAD and $2 \cdot 10^{-5}$ for glutamate. According to criterion 3.2, $\eta_{S,e}$ is unity for both NAD and glutamate, and external transport effects are negligible. Thus, the substrate concentrations at the exterior surface of the support bead and in the bulk fluid were both equal to $[S]_o$.

The observable Thiele modulus, Φ, is a useful indicator of whether or not the kinetic activity of Sepharose-immobilized GluDH was limited by internal diffusion.

$$\Phi_S \equiv \frac{v_o}{D_{S,pore}\,[S]_o}\left(\frac{V_B}{A_B}\right)^2 \begin{cases} < 0.3, & \text{diffusional effects are negligible;} \\ > 3.0, & \text{activity is diffusion limited.} \end{cases} \tag{3.8}$$

In this equation, $D_{S,pore}$ is the diffusion coefficient of the substrate in a porous support; V_B, the volume of the support bead containing enzyme; and A_B, the average surface area of the bead in this occupied region [20].

For the experimental conditions described in this paper, factors which enter into Φ were estimated using information from several sources. Determining $(V_B/A_B)^2$ required the distribution of GluDH within Sepharose 4B. It was noted in Chapter 1 that the immobilized enzyme is limited to a spherical shell, 8 μm thick, on the exterior of the Sepharose bead. For this distribution, $(V_B/A_B)^2$ is approximately 64 μm^2. The ratio of the diffusion coefficient in Sepharose 4B, $D_{S,\,pore}$, to that in an aqueous solution, D_S , is 0.67 for N-acetyl-L-tyrosine ethyl ester [12]. Since the molecular weight of glutamate is smaller than that of this ester, 0.67 represents the lower limit of this ratio for glutamate. Thus, a $D_{Glu,\,pore}$ value of $4.9 \cdot 10^{-6} cm^2/sec$ was used in Φ_{Glu} calculations. The ratio of $D_{NAD,\,pore}$ to D_{NAD} should be less than 0.67 since NAD is a larger molecule than N-acetyl-L-tyrosine ethyl ester. Regan et al. used a value of 0.2 in their work with porous DEAE-cellulose beads with a mean particle diameter of 40 μm [17].

With this data, Φ_{Glu} was found to be no larger than $2 \cdot 10^{-5}$. With a $(D_{NAD,\,pore}/D_{NAD})$ ratio of 0.2, Φ_{NAD} never exceeded $2 \cdot 10^{-4}$. Since both Φ_{NAD} and Φ_{Glu} are dramatically less than 0.3, Equation 3.8 indicates that the rates of NAD and glutamate consumption were not limited by internal diffusion in the experiments described in this paper.

For a reaction that generates hydrogen ions, there is another aspect of mass transport to consider: a pH change within the Sepharose bead. Such a change in the immediate vicinity of the immobilized enzyme would profoundly affect its catalytic activity.

Bailey's expression for a chemical reaction occurring within a porous catalyst was used to relate the internal and external hydrogen ion concentrations [21].

$$[X_i]_r = [X_i]_R + \frac{\nu_i}{D_{H^+,\,pore}} y_r. \tag{3.9}$$

Here, r is a position variable and is equal to R at the surface of the bead; $[X_i]_r$, the concentration of the ith reacting species, X_i, at r; ν_i, the stoichiometric coefficient for species i; and y_r, the extent of reaction at r.

When NAD was the limiting substrate as in Figures 3.3 and 3.4, $[H^+]$ was related to [NAD] with Equation 3.9 [22].

$$[H^+]_r = [H^+]_R + \frac{D_{NAD,\,pore}}{D_{H^+,\,pore}} ([NAD]_R - [NAD]_r). \tag{3.10}$$

To maximize $[H^+]_r$, $[\mathrm{NAD}]_r$ was set equal to zero. With a D_{H^+} value of $1 \cdot 10^{-4}$ cm^2/sec [23] and a $(D_{H^+,\,pore}/D_{H^+})$ ratio of 0.67, the maximum value of $[H^+]_r$ equaled $1.38 \cdot 10^{-5}$ M when $[H^+]_R$ was 10^{-8} M and $[\mathrm{NAD}]_R$ was 1.4 mM.

This maximum value was incorporated into a set of coupled dissociation equations. At equilibrium,

$$K_i = \frac{[H^+]_r ([X_i']_r - \delta_i)}{([HX_i']_r + \delta_i)} \qquad for\ i = 1\ to\ n, \tag{3.11}$$

and

$$[H^+] = 1.38 \cdot 10^{-5}\ M - \sum_{i=1}^{n} \delta_i. \tag{3.12}$$

In these expressions, δ_i and K_i are the extent of association and dissociation constant for species i, respectively. In addition, $[X_i']_r$ is the initial concentration of the ith species at r in the buffered solution for our kinetic assays. Unlike

X_i, X_i' includes nonreacting species. There are a total of n such species in the buffered solution. To solve Equations 3.11 and 3.12, the following species and corresponding K_i values were used: HPO_4^{2-}, $6.23 \cdot 10^{-8}$ M [24]; EDTA, $7.76 \cdot 10^{-7}$ M and $6.76 \cdot 10^{-11}$ M [25]; glutamate, $1.99 \cdot 10^{-10}$ M [26]; and NH_3, $5.60 \cdot 10^{-10}$ M [24]. Other species with K_i's above 10^{-5} M, such as NAD [27], and below 10^{-11} M, such as PO_4^{3-} [24], had a negligible effect on $[H^+]$. With these constants, we determined that the pH within the Sepharose bead changed by less than 0.01 unit during our kinetic assays. The same result was obtained when glutamate was considered as the limiting substrate.

In summary, the above analyses show that all kinetic data presented in this paper represent the intrinsic catalytic properties of the enzyme and are not disguised or disturbed by external or internal mass transport limitations.

Kinetic models

To date, two kinetic models have been used to analyze free and immobilized GluDH data. By deleting terms from a general rate equation for a multi-site enzyme, Engel and Ferdinand were able to obtain an expression which models the kinetic behavior of free GluDH as a function of NAD concentration, including the abrupt activation [3]. In the second model, each linear region in Lineweaver-Burk plots of inverse rate vs. inverse substrate concentration are fitted to a steady-state Michaelis-Menten expression for a two substrate reaction [6,9].

Neither of these two models accounts for the effects that structural heterogeneity, conformational change and a second, non-catalytic NAD binding site

have on substrate activation. Only when these three factors have been quantitatively characterized will such a detailed model of the activation phenomenon be feasible.

In the past, the majority of GluDH kinetic data was fitted to a Michaelis-Menten expression. The same will be done here to facilitate a comparison of results.

Results

pH profile of free and immobilized GluDH

The pH dependence of GluDH activity is displayed in Figure 3.1. This graph reveals that the pH profiles for free and immobilized GluDH are very similar above pH 7.4. In particular, the activities of both enzymes are maximized at pH 8.0. The similarity of these two curves supports our argument that the kinetic activity of immobilized GluDH is free of mass transport effects at pH 8.0 [28]. Lastly, the pH profile for immobilized GluDH is not significantly affected by separating the enzyme from the support with a C_6 spacer arm or by increasing the protein loading on the support.

NAD activation

Engel and Dalziel have thoroughly examined NAD activation in the free enzyme [6]. When GluDH is exposed to 87 mM sodium phosphate buffer (pH 8.0) containing 10 μM EDTA and 8 mM glutamate at 25°C, it generates four linear regions in Lineweaver-Burk plots over a concentration range of 0.2 μM to 2.0 mM NAD. These regions are separated by sharp discontinuities. Moreover, both the rate and NAD dissociation constants are larger in linear regions corresponding to higher NAD concentrations.

The kinetic study of Engel and Dalziel strongly suggests that the formation of the NAD(P)-Glu-GluDH ternary complex is necessary for activation [6]. With 0.3 mM glutamate in a phosphate buffer (pH 7.0), Lineweaver-Burk plots are linear for the free enzyme over a NADP concentration range of 2 μM to 1.0 mM. Under these conditions, K_{Glu} , K_{NADP} and $K_{Glu.\,NADP}$ are 6.61, 0.75 and 0.65 mM, respectively [6].[1] In the presence of 0.3 mM glutamate and 1.0 mM

NADP, only 21% of the enzyme is in the ternary complex. When the glutamate concentration is raised to 50 mM, 91% of the biocatalyst exists as NADP-Glu-GluDH, and sharp discontinuities are visible in the Lineweaver-Burk plots.

In this work, the effects of immobilization on NAD activation were investigated near a single discontinuity in the Lineweaver-Burk plot for free GluDH. In particular, the discontinuity occurring at the largest NAD concentration, 0.5 mM, was examined. A phosphate buffer (pH 8.0) containing 50 mM glutamate was employed in order to provide a high percentage of the free and immobilized enzyme in the NAD-Glu-GluDH complex. Lineweaver-Burk plots obtained under these conditions show that both free (Fig. 3.2) and immobilized GluDH (Fig. 3.3) are activated by NAD. This phenomenon was examined with four different combinations of protein loadings and Sepharose supports. These are listed in Table 3.1.

NAD activation can be characterized by the shape and position of the discontinuity in the Lineweaver-Burk plot; the apparent Michaelis-Menten dissociation constant, ${K^N}_{m,\,app}$, for NAD; and the apparent rate constant, ${k^N}_{app}$, for NAD. The following paragraphs are devoted to studying the effect of immobilization on NAD activation from these three perspectives.

When NAD is the varied substrate, immobilization of GluDH broadens the discontinuity in Lineweaver-Burk plots (Fig. 3.3). For the free enzyme, this break occurs abruptly. The activation scenario for immobilized GluDH is characterized by a broad transition region containing two inflection points. Specifically, the curves in Figure 3.3 have decreasing slopes at low $[\mathrm{NAD}]^{-1}$ values within the transition region, pass through an inflection point, have increasing slopes at intermediate $[\mathrm{NAD}]^{-1}$, pass through a second inflection point, and

have decreasing slopes again at high $[NAD]^{-1}$. For example, these inflection points occur at 0.28 and 0.35 mM NAD in Figure 3.3b. (For the low loading of GluDH on CH-activated Sepharose, there are insufficient data at high concentrations of NAD to observe the second inflection point and the subsequent decreasing slope.)

Teipel and Koshland noticed that several free enzymes had elongated activation regions containing two inflection points [29]. The data for the low loading of GluDH on CNBr-activated Sepharose 4B were replotted in the form of Teipel's and Koshland's graphs in order to compare immobilized GluDH (Fig. 3.4) to these free enzymes. An examination of Figure 1 in their paper reveals that our bovine liver GluDH-Sepharose conjugate, *E. coli* CTP synthetase, *E. coli* W phosphoenolpyruvate carboxylase [29] and honeybee glyceraldehyde 3-phosphate dehydrogenase [30] have similar activation patterns. *E. coli* B ADP-glucose pyrophosphorylase also exhibits this type of behavior when activated by ATP in the presence of Mg^{2+} [31]. Furthermore, free *Blastocladiella emersonii* GluDH undergoes an elongated activation, but the transition region is not as pronounced as in the plots from the other enzymes [29].

The position of the transition region varies for the immobilized enzyme preparations represented in Figure 3.3. When the enzyme is covalently coupled to CNBr-activated Sepharose, the transition region initiates at 0.28 mM NAD. This region ends, on average, at 0.525 mM, the break point for NAD activation of free GluDH. Separating the enzyme from the Sepharose support with a C_6 spacer arm causes activation to occur at lower NAD concentrations. For example, the transition region ends at 0.36 mM NAD for the biocatalyst with 4.9 mg of functional protomers per gram of CH-activated Sepharose.

We now focus on a quantitative characterization of NAD activation with ${K^N}_{m,\,app}$ and ${k^N}_{app}$. For comparison, these constants are defined below in terms of rate parameters used by Engel and Dalziel [6]. If

$$\frac{[e_f]}{v} = \phi_o + \frac{\phi_1}{[S_1]} + \frac{\phi_2}{[S_2]} + \frac{\phi_{1\,2}}{[S_1]\,[S_2]} \quad , \tag{3.13}$$

then

$${K^{S_1}}_{m,\,app} = \frac{\left(\phi_1 + \frac{\phi_{1\,2}}{[S_2]}\right)}{\left(\phi_o + \frac{\phi_2}{[S_2]}\right)} \tag{3.14}$$

and

$${k^{S_1}}_{app} = \left(\phi_o + \frac{\phi_2}{[S_2]}\right)^{-1} \tag{3.15}$$

when $[S_2]$ is held constant. Here, $[e_f]$ is the initial concentration of functional protomers; v is the initial steady-state velocity; $[S_i]$ is the concentration of substrate i; and the ϕ's are kinetic coefficients. In addition, apparent rate constants were adjusted to a molecular weight of $5.6 \cdot 10^4$ for the enzyme. Using this procedure, we determined that Engel's and Dalziel's free GluDH preparation [6] was characterized by ${K^N}_{m,\,app}$ and ${k^N}_{app}$ values of 0.19 mM and 553 mole NADH/mole e_f per min , respectively, in the linear region from 0.2 to 0.5 mM NAD. The ratio, $({K^N}_{m,\,app}/{k^N}_{app})$, obtained in their experiments was the same as we observed. However, both their ${K^N}_{m,\,app}$ and ${k^N}_{app}$ were greater than the values we obtained (0.13 mM and 377 mole NADH/mole e_f per min , respectively) by a factor of 1.5 (Table 3.1). Equations 3.14 and 3.15 show that $({K^N}_{m,\,app}/{k^N}_{app})$ is independent of ϕ_0 which is the inverse of the rate constant at an infinite glutamate concentration. This suggests that the difference in the individual kinetic parameters and the conservation of their ratio reflect a larger percentage of inactive protomers in our GluDH preparation. This is possible:

Engel and Dalziel purchased GluDH as a crystalline suspension in a $(NH_4)_2SO_4$ solution, while we bought GluDH dissolved in a 50% glycerol solution.

Qualitative changes in Figure 3.3 correspond to quantitative changes in $K^N{}_{m,\,app}$ and $k^N{}_{app}$. For simplicity, this analysis will focus on NAD activation of the immobilized enzyme preparation containing 2.8 mg of functional protomers per gram of CNBr-activated Sepharose (Fig. 3.3b). Within the transition region, both kinetic parameters are increased as the NAD concentration is raised from 0.22 to 0.4 mM: $K^N{}_{m,\,app}$ increases from 0.04 to 0.8 mM, while $k^N{}_{app}$ changes from 300 to 1 061 mole NADH/mole e_f per min (Table 3.2). This feature of $K^N{}_{m,\,app}$ increasing with [NAD] is referred to as negative cooperativity [2,6] and is characteristic of NAD activation of free GluDH (Table 3.1). In the 0.4 to 0.55 mM NAD region, the dissociation and rate constants are reduced to 0.31 mM for $K^N{}_{m,\,app}$ and 606 mole NADH/mole e_f per min for $k^N{}_{app}$. Although these values are less than those corresponding to the 0.28 to 0.4 mM NAD region, they are still greater than those in the 0.22 to 0.28 mM NAD segment. Near the end of the transition region, the immobilized GluDH preparation experiences a second negatively cooperative activation at 0.55 mM NAD. Combined, this series of changes in $K^N{}_{m,\,app}$ and $k^N{}_{app}$ produces an overall negatively cooperative activation: the kinetic parameters increase from 0.04 to 1.43 mM for $K^N{}_{m,\,app}$ and from 300 to 1 338 mole NADH/mole e_f per min for $k^N{}_{app}$.

One of the benefits of immobilization is that it can enhance the apparent rate constant. Specifically, immobilized enzyme preparations containing 2.8 mg of functional protomers per gram of CNBr-activated Sepharose and 10.2 mg of functional protomers per gram of CH-activated Sepharose have $k^N{}_{app}$'s equal to 1 338 and 1 101 mole NADH/mole e_f per min , respectively (Table 3.1). This is,

on average, 2.0 times the free enzyme value. This activity enhancement is not a consequence of the assay conditions since all kinetic measurements were made at pH 8.0 (which maximizes the activity of both free and immobilized GluDH) and at 25°C (Fig. 3.1). Nor is the enhancement a consequence of the active site titration. As indicated earlier in this paper, an overestimate of the number of catalytically functional protomers in a GluDH-Sepharose preparation will only make its true specific rate constant even larger than the reported value. Thus, the enhanced k values are intrinsic to the immobilized enzyme preparations cited.

Glutamate activation

To complement NAD activation data, GluDH kinetics were studied as a function of the glutamate concentration in solution. With 2 mM NAD, glutamate concentrations were varied from approximately 0.5 to 10 mM in the free and immobilized GluDH kinetic assays (Table 3.3, & Figs. 3.5 & 3.6). As in the NAD activation experiments, these concentrations were chosen to maximize the amount of enzyme in the ternary complex. At pH 8.0, the glutamate experiments show that free GluDH exhibits classical Michaelis-Menten behavior below 1.4 mM glutamate and inhibition above this concentration (Fig. 3.5). In their kinetic investigation of free GluDH, Engel and Dalziel observed inhibition above 50 mM glutamate when the enzyme was exposed to 140 μM NADP in a phosphate buffer (pH 7.0) [6]. They suggested that inhibition is caused by the formation of the abortive complex, NAD(P)H-Glu-GluDH. Immobilization postpones or eliminates inhibition (Fig. 3.6). This delay could be due to a decrease in the binding affinity of either NADH or glutamate for the abortive complex.

Besides postponing inhibition, immobilization produces varying degrees of glutamate activation (Fig. 3.6). The sharp discontinuities in Figure 3.6 resemble NAD activation of free GluDH (Fig. 3.2). These discontinuities occur at approximately 1.6 mM glutamate, which is near the transition concentration (1.4 mM) from Michaelis-Menten behavior to inhibition in the free enzyme. The difference in the slopes of the two intersecting lines, $\Delta\ (K^G{}_{m,\,app}/k^G{}_{app})$, quantifies the extent of activation in each GluDH-Sepharose preparation. This Δ term ranges from zero (Michaelis-Menten kinetics) for a gram of CNBr-activated Sepharose loaded with 2.8 mg of functional protomers to 2.95 μM Glu · mole e_f · min/mole NADH for a higher loading on the same support (Table 3.3).

Two patterns exist in Table 3.3. First, glutamate activation increases both $K^G{}_{m,\,app}$ and $k^G{}_{app}$. Recall that this negative cooperativity also characterizes NAD activation of the free enzyme (Table 3.1). Second, a correlation exists between the degree of activation and the apparent rate constant in both the 0.5 to 1.6 mM and 1.6 to 10 mM glutamate regions: $\Delta\ (K^G{}_{m,\,app}/k^G{}_{app})$ is greater for smaller $k^G{}_{app}$. In addition, activation only occurs in those immobilized GluDH preparations that have $k^G{}_{app}$ values that are less than 596 mole NADH/mole e_f per min , which is the apparent rate constant for the free enzyme.

Stability

Another possible advantage of immobilization is reduction in enzyme deactivation rates. The operational stability of immobilized GluDH was evaluated by washing 3 mg of beads containing 10.2 mg of functional protomers per gram of CH-activated Sepharose with 25 ml of 87 mM sodium phosphate (pH 8.0)

containing 10 μM EDTA after each of a sequence of kinetic assays. Washing served to remove substrates and products from the porous Sepharose beads. After thirteen assays, the support was still fully active within experimental error. It should be noted that exposing the immobilized biocatalyst to air between assays was minimized. Keeping the beads dry for a prolonged period of time will most likely deactivate the enzyme.

Discussion

The objective of this research is to better understand which structural properties of GluDH are responsible for substrate activation. To this end, immobilization was used to alter the activation patterns of this enzyme. In the following section, these kinetic changes will be analyzed in terms of structural properties of bovine liver GluDH and activation patterns in several other free allosteric enzymes and GluDH systems. Combined, this information will provide insight into structure-function relationships which generate substrate activation.

NAD activation

Sepharose-immobilization causes NAD activation to change from being abrupt to being elongated and containing two inflection points. With a kinetic model, Teipel and Koshland determined that two criteria suffice to generate this elongated activation in a homogeneous enzyme population: the enzyme must have more than two substrate binding sites; and the relative magnitudes of the substrate binding constants or intrinsic rate constants must decrease, at first, and then increase as the enzyme becomes saturated with substrate. Substrate-induced conformational change may produce this effect [29]. The changes in kinetic constants that Teipel and Koshland described call to mind the pattern in Table 3.2. Unfortunately, a direct comparison of the two is not possible since both $K^N{}_{m,\,app}$ and $k^N{}_{app}$ are complex functions of kinetic coefficients (Equations 3.14 & 3.15). However, such changes in our kinetic parameters could reflect conformational change. Teipel and Koshland also mentioned that a heterogeneous mixture of enzymes can generate the elongated activation pattern; however, they did not discuss the criteria for activation in this system [29]. Teipel's and Koshland's findings suggest that immobilization alters

NAD activation of GluDH by affecting conformational change and structural heterogeneity.

In modeling NAD activation of free GluDH, Engel and Ferdinand found that the abrupt transition reflects a decrease followed by an increase in the kinetic activity or substrate binding affinity as the enzyme becomes saturated with substrate [3]. This combination of negative and positive interactions also resembles the pattern described by Teipel and Koshland and that in Table 3.2. This similarity suggests that this pattern of change exists in free GluDH and is enhanced by immobilization.

To the best of our knowledge, a broad activation region has not been observed in previous studies of immobilized GluDH. Examining other GluDH coupling procedures exposed differences in experimental conditions that could affect activation. Of all the immobilization protocols given in the literature, the one that most closely resembles ours was developed by Havekes et al. [9]. Using GluDH attached to CNBr-activated Sepharose 4B, they observed a sharp discontinuity in the Lineweaver-Burk plot at 0.25 ± 0.05 mM NAD. Their break point occurs at approximately the beginning of our transition region. There are two factors in the coupling procedure given by Havekes et al. that could have influenced the shape of the discontinuity. First, substrates and cofactors such as NAD(P)H, α-ketoglutarate, ADP and GTP were included in their coupling buffer. Since many of these biochemicals contain primary amino groups, they most likely attached to Sepharose along with the enzyme. Second, their loading of total protein on the support was less than ours by a factor of 10 to 30. Both of these differences would tend to make NAD activation in immobilized GluDH approach that in the free enzyme. Compared to crowded conditions on

a support, low loadings could ease restrictions on conformational change. With substrates and cofactors present during immobilization, the biocatalyst could be attached to Sepharose in a form that is more conducive to NAD activation. It should be noted that the reason why the protocol developed by Havekes et al. was not adopted for this research stems from our desire to link structural and kinetic changes in GluDH. The high loadings achieved with our protocol were required for structural analysis of the enzyme with ESR spectroscopy.

Glutamate activation

Our findings show that different loadings of GluDH on CNBr- and CH-activated Sepharose produce varying degrees of glutamate activation. Yet under the same experimental conditions, the free enzyme is inhibited by glutamate. The intensity of the Sepharose-induced activation is inversely related to the apparent rate constant of the immobilized biocatalyst. In our system, only those GluDH-Sepharose preparations with $k^G{}_{app}$ values less than that of the free enzyme exhibited activation. Moreover, glutamate activation in immobilized GluDH resembles NAD activation in the free enzyme: both are abrupt and increase the two kinetic parameters, $K_{m,\,app}$ and k_{app}, as the substrate concentration is raised (negatively cooperative activation).

Other researchers have observed that immobilization induces glutamate activation of bovine liver GluDH. When the enzyme is coupled to CNBr-activated Sepharose 4B in a phosphate buffer (pH 7.2) containing substrates and cofactors, Havekes et al. reported that GluDH is abruptly activated at 25°C by approximately 3 mM glutamate in 100 mM sodium phosphate buffer (pH 8.0) containing 1.0 mM NAD, 0.1 mM EDTA and 0.5 mM β-mercaptoethanol [9]. Visual examination of their Lineweaver-Burk plots reveals that the correlation

noted here between $k^G{}_{app}$ and the degree of activation is valid for their system.[2] Also, this allosteric response is negatively cooperative. There are insufficient data to quantify this negative cooperativity, degree of activation or $k^G{}_{app}$ for free GluDH under ATP-free experimental conditions. When the enzyme is immobilized to CNBr-activated Sepharose 4B in a borate buffer (pH 9.0) instead of a phosphate buffer (pH 7.2), glutamate activation remains abrupt and negatively cooperative [9]. However, the correlation is reversed: both the apparent rate constant and the activation intensity decrease simultaneously. Havekes et al. believed that NAD and glutamate activation were intrinsic to their immobilized enzyme and were not primarily caused by diffusional limitations. The reasons for this conclusion are listed in their paper. According to Julliard et al., thin films of collagen bound GluDH become activated at approximately 1 mM glutamate in 0.02 M potassium phosphate buffer (pH 8.0) containing 0.5 mM NAD, 0.5 mM EDTA and 0.5 mM β-mercaptoethanol at 28°C [32]. Under the same conditions, they did not observe this behavior in the free biocatalyst. Again, this activation is negatively cooperative. There are insufficient data to correlate $k^G{}_{app}$ to the degree of activation, to quantify the negative cooperativity, and to calculate $k^G{}_{app}$ for the free enzyme. The influence of substrate diffusion on the results for this collagen system was not discussed.

Glutamate activation is not limited to immobilized GluDH systems; it has been observed in kinetic studies of the free enzyme. In each of the following examples, this activation is negatively cooperative and is quantified were possible. Unlike the abrupt activation depicted in Figure 3.6, Barton and Fisher detected a very gradual activation over the concentration range of 0.2 to 10 mM glutamate when NAD concentrations are either 13, 21, 43 or 85 μM in 0.1 M phosphate buffer (pH 8.0) at 27°C [33]. As mentioned earlier, Engel and

Dalziel did not observe glutamate activation of the free enzyme. Barton and Fisher suggested that the reason for this is that Engel and Dalziel monitored GluDH activity over narrower substrate and cofactor concentration ranges. Hornby and Engel reported another case of substrate activation with the free enzyme [34]. It occurs abruptly at an amino acid concentration of approximately 2 mM when glutamate is replaced by either L-*threo*-γ-methylglutamate or L-γ-methyleneglutamate in 0.11 M potassium phosphate buffer (pH 7.0 or 8.0) containing 200 μM NAD at 25°C. This activation concentration is similar to ours, 1.4 mM. Examination of their Lineweaver-Burk plot shows that, like our immobilized GluDH, their activated systems have $k^G{}_{app}$ values greater than that of their unactivated glutamate reference in the region from 2 to 4 mM amino acid. Hornby and Engel were the first to note that activation intensity is inversely related to $k^G{}_{app}$. Finally, free *Blastocladiella* GluDH, a tetramer, generates Lineweaver-Burk plots with sharp discontinuities at 100 mM glutamate [35]. In this enzyme, glutamate activation occurs when a low concentration of NAD, on the order of 1 mM, is present in 0.2 M Tris-chloride buffer (pH 9.0). Activation is eliminated when the NAD concentration is 3 mM or higher. A Lineweaver-Burk plot from this *Blastocladiella* GluDH study reveals that the activated GluDH systems have $k^G{}_{app}$ magnitudes greater than that of the unactivated enzyme. The range of $k^G{}_{app}$ values for the activated systems is too narrow to correlate $k^G{}_{app}$ to the degree of activation. Because these trends in $k^G{}_{app}$ occur in many GluDH systems besides our own, they are not a byproduct of our immobilization protocol; rather, these trends appear to be intrinsic properties of amino acid activation in GluDH.

Structure-function relationships

Structural heterogeneity, conformational change and a second, non-catalytic NAD binding site have been mentioned in the literature as potential sources for substrate activation of free GluDH [2,3]. In the following, the impact of these structural properties on activation will be analyzed in light of the findings in this paper.

Kinetic models of NAD activation of free GluDH [3] and elongated activation of allosteric oligomers [29] predict that activation can be produced by a heterogeneous mixture of two or more structural forms of GluDH. ESR spectra in Chapter 1 suggest that immobilized GluDH is structurally heterogeneous. Two protomers may have a conformation different from that of the other four. This conformational distribution is the same for all four GluDH-Sepharose preparations in Tables 3.1 and 3.3. If this heterogeneity is present in free GluDH, then it is less pronounced. This investigation with the ketone label is supported by another ESR study with ClHgBz-TEMPO (Chapter 2). The spectrum of Sepharose-immobilized GluDH spin labeled with this mercuric probe also suggests structural heterogeneity. Although the heterogeneity is not clearly distinguishable in the spectrum of the free enzyme, the two line shapes are sufficiently compatible that the heterogeneity could exist in the free enzyme and be enhanced by immobilization. Perhaps the more pronounced substrate activation of immobilized GluDH reflects increased heterogeneity.

Together, kinetic and spectroscopic studies of free GluDH suggest that conformational change is related to activation [2,4]. Conformational change is triggered by the formation of the ternary complex, NAD-Glu-GluDH [2,4]. The

potential of immobilization to modify conformational change is great. During immobilization, dioxane separates aggregated GluDH into active hexamers. Subsequently, the individual hexamers are attached to Sepharose via primary amino groups (Chapter 1). Probably, the hexamer binds to the support in several places which may dramatically affect conformational change. In Chapter 2, ESR spectra of GluDH spin labeled with ClHgBz-TEMPO show that Sepharose-immobilization eliminates conformational change induced by GTP and NADPH and profoundly alters that induced by α-ketoglutarate. The fact that immobilization affects both conformational change and activation indicates that the relationship between the two is valid.

This activation scenario for GluDH is consistent with structure-function relationships for other free oligomeric enzymes which have activation properties similar to those of Sepharose-immobilized GluDH. Honeybee glyceraldehyde 3-phosphate dehydrogenase exists in two structural forms, stable and metastable, which can be separated by polyacrylamide gel electrophoresis in sodium dodecyl sulfate [30]. The conversion from the stable to metastable state most likely produces glyceraldehyde 3-phosphate activation in the presence of NAD. These two substrates induce the conversion through disulfide bond formation. *E. coli* CTP synthetase undergoes conformational change when it reacts with a substrate analogue, 6-diazo-5-oxonorleucine. When half of the active sites are labeled with this analogue, glutamine activity is abolished in the vacant as well as the labeled active sites. This half-of-the-sites reactivity reflects a transmission of conformational change between protomers [36]. *E. coli* W phosphoenolpyruvate carboxylase exists in multiple conformational states. These different states were detected by monitoring the reactivity of essential -SH groups, degree of heat inactivation and fluorescence emission from a hydrophobic probe bound to the

enzyme. Conformational change between these states is induced by allosteric effectors, such as acetyl-coenzyme A [37,38].

In addition to confirming the existence of these two relationships, this research refutes a previous hypothesis about substrate activation of GluDH. We propose that a second NAD binding site per protomer is not a prerequisite for NAD activation [3]. If this second site were required, then all other free enzymes which exhibit GluDH-like activation would have two or more binding sites per protomer for the activating substrate. This is not the case. *E. coli* CTP synthetase is a tetramer in the presence of saturating concentrations of ATP and UTP, and a dimer in their absence. Each protomer of CTP synthetase has a single glutamine binding site [36]. Saturation of these binding sites with glutamine induces an elongated activation similar to NAD activation of Sepharose-immobilized GluDH [29].

This research has also demonstrated that NAD activation of bovine liver GluDH is not an artifact of ADP contamination. It has been suggested in the literature that NAD activation of *Blastocladiella* GluDH is induced by an AMP-like substance in the NAD preparation rather than by NAD itself [39]. *Blastocladiella* and bovine liver GluDH are analogous enzyme systems: AMP is an activator of the former; ADP, of the latter. This analogy suggests that ADP contamination of our NAD preparation might have produced the NAD activation in Figures 3.2, 3.3, and 3.4. This is not likely. Our NAD was purchased from Boehringer Mannheim Biochemicals and was classified by this company as grade I. For a NAD preparation to have this classification, NAD must be present in amounts greater than or equal to 97% as determined by absorbance measurements at 260 nm, enzymatic assay and CN complex formation. A Karl Fischer

reagent was used to show that the other 3% is water. Also, grade I preparations of NAD contain less than 0.1% AMP as detected with an enzymatic assay (personal communication with M. Gatton at Boehringer Mannheim). Since the NAD that we used was so pure, it is extremely unlikely that NAD activation is produced by a contaminant.

This research represents a three-fold approach to investigating allosteric regulation. Specifically, results from kinetic and ESR studies (Chapters 1 and 2) were combined to provide insight into the relationship between activation and GluDH structure. By immobilizing GluDH, its kinetic and structural properties became more pronounced than in the free enzyme. In this way, the central roles of structural heterogeneity and conformational change in activation were demonstrated. In the future, this three-fold approach could be used to explore allosteric regulation in the other free enzymes cited in this work which exhibit structure-function relationships similar to those of GluDH.

Footnotes

1 K_S is the dissociation constant of S from the S-GluDH complex. Similarly, $K_{S_1,\,S_2}$ signifies the dissociation of S_1 from the S_1-S_2-GluDH complex.

2 Unlike $K^S{}_{m,\,app}$, $k^S{}_{app}$ is a function of how an immobilized enzyme population is characterized. A k^S value based on the total protein content in a support will differ from the same k^S value derived from only the functional enzymes in the same system. Since all of the immobilized GluDH systems found in the literature have been characterized by only the total protein content, a direct, quantitative comparison of rate constants from these systems with ours is not possible. However, changes in the relative magnitudes of a set of $k^S{}_{app}$ values can be compared.

References

1 Sund, H., Markau, K. and Koberstein, R. (1975) in Biological Macromolecules, Subunits in Biological Systems, Part C, vol. 7 (Timasheff, S. N. and Fasman, G. D., eds.), pp. 225-287, Marcel Dekker, New York

2 Bell, E. T., LiMuti, C., Renz, C. L. and Bell, J. E. (1985) Biochem. J. 225, 209-217

3 Engel, P. C. and Ferdinand, W. (1973) Biochem. J. 131, 97-105

4 Chen, S.-S., Engel, P. C. and Bayley, P. M. (1977) Biochem. J. 163, 297-302

5 Zantema, A., Vogel, H. J. and Robillard, G. T. (1979) Eur. J. Biochem. 96, 453-463

6 Engel, P. C. and Dalziel, K. (1969) Biochem. J. 115, 621-631

7 Wootton, J. C. (1974) Nature 252, 542-546

8 Horton, H. R., Swaisgood, H. E. and Mosbach, K. (1974) Biochem. Biophys. Res. Commun. 61, 1118-1124

9 Havekes, L., Bückmann, F. and Visser, J. (1974) Biochim. Biophys. Acta 334, 272-286

10 (1983) Affinity Chromatography: Principles and Methods, pp. 11-33, Pharmacia Fine Chemicals, Sweden

11 Ford, J. R., Lambert, A. H., Cohen, W. and Chambers, R. P. (1972) Biotechnol. Bioeng. Symp. 3, 267-284

12 Clark, D. S. and Bailey, J. E. (1983) Biotechnol. Bioeng. 25, 1027-1047

13 Zantema, A., De Smet, M.-J. and Robillard, G. T. (1979) Eur. J. Biochem. 96, 465-476

14 Carberry, J. J. (1976) Chemical and Catalytic Reaction Engineering, pp. 196-209, McGraw-Hill, New York

15 Hill, C. G., Jr. (1977) An Introduction to Chemical Engineering Kinetics and Reactor Design, pp. 474-476, John Wiley & Sons, New York

16 Weast, R. C. (ed.) (1978) Handbook of Chemistry and Physics, pp. C318, F11 & F51, CRC Press, West Palm Beach, FL

17 Regan, D. L., Lilly, M. D. and Dunnill, P. (1974) Biotechnol. Bioeng. 16, 1081-1093

18 Longsworth, L. G. (1953) J. Amer. Chem. Soc. 75, 5705-5709

19 Thoenes, D., Jr. and Kramers, H. (1958) Chem. Eng. Sci. 8, 271-283

20 Bailey, J. E. and Ollis, D. F. (1977) Biochemical Engineering Fundamentals, pp. 395-398, McGraw-Hill, New York

21 Bailey, J. E. (1973) Chem. Eng. Sci. 28, 1417-1422

22 Bailey, J. E. and Chow, M. T. C. (1974) Biotechnol. Bioeng. 16, 1345-1357

23 Ruckenstein, E. and Kalthod, D. G. (1982) Biotechnol. Bioeng. 24, 2357-2382

24 Dickerson, R. E., Gray, H. B. and Haight, G. P., Jr. (1974) Chemical Principles, p. 179, Benjamin/Cummings, Menlo Park, California

25 Martell, A. E. and Smith, R. M. (1982) Critical Stability Constants, vol. 5, p. 75, Plenum Press, New York

26 Wood, W. B., Wilson, J. H., Benbow, R. M. and Hood, L. E. (1981) Biochemistry: A Problems Approach, p. 15, Benjamin/Cummings, Menlo Park, California

27 Serjeant, E. P. and Dempsey, B. (1979) Ionisation Constants of Organic Acids in Aqueous Solution, p. 745, Pergamon Press, New York

28 Chang, H. N. and Joo, I. S. (1985) Chem. Eng. Commun. 34, 15-25

29 Teipel, J. and Koshland, D. E., Jr. (1969) Biochemistry 8, 4656-4663

30 Gelb, W. G., Brandts, J. F. and Nordin, J. H. (1974) Biochemistry 13, 280-287

31 Gentner, N. and Preiss, J. (1968) J. Biol. Chem. 243, 5882-5891

32 Julliard, J. H., Godinot, C. and Gautheron, D. C. (1971) FEBS Lett. 14, 185-188

33 Barton, J. S. and Fisher, J. R. (1971) Biochemistry 10, 577-585

34 Horby, D.P., Engel, P. C. and Hatanaka, S.-I. (1983) Int. J. Biochem. 15, 495-500

35 LéJohn, H. B. and Jackson, S. (1968) J. Biol. Chem. 243, 3447-3457

36 Levitzki, A., Stallcup, W. B. and Koshland, D. E., Jr. (1971) Biochemistry 10, 3371-3378

37 Teraoka, H., Izui, K. and Katsuki, H. (1974) Biochemistry 13, 5121-5128

38 Yoshinaga, T. (1976) Biochim. Biophys. Acta 452, 566-579

39 Sanner, T. (1971) Biochim. Biophys. Acta 250, 297-305

Table legends

Table 3.1 Kinetic parameters for NAD activation. The following parameters were evaluated from the linear regions in Figures 3.2 and 3.3 using a least-squares linear regression fitting.

Table 3.2 Effect of NAD activation on kinetic parameters. Kinetic data from the NAD activation of 2.8 mg of functional protomers per gram of CNBr-activated Sepharose (Fig. 3.3b) were divided into four pseudo-linear regions. Then, $K^N_{m,\,app}$ and k^N_{app} were evaluated as described in the legend of Table 3.1.

Table 3.3 Kinetic parameters for glutamate activation. The following parameters were evaluated from the linear regions in Figures 3.5 and 3.6 as described in the legend of Table 3.1.

Table 3.1

Support Type	Loading (mg e_f/g bead)	Linear NAD Region (mM)	Break Point (mM)	$K^N_{m,\,app}$ (mM)	k^N_{app} (mole NADH/ mole e_f per min)
None[a,b]	—	0.20 – 0.50	0.50	0.19	553
None[a]	—	0.22 – 0.53	0.53	0.13	377
		0.53 – 2.00		0.56	610
CNBr-activated Sepharose	17.0	0.50 – 1.40	0.28 – 0.50	1.01	445
CNBr-activated Sepharose	2.8	0.55 – 1.40	0.28 – 0.55	1.43	1 338
CH-activated Sepharose	10.2	0.40 – 1.40	0.25 – 0.40	1.53	1 101
CH-activated Sepharose	4.9	0.36 – 1.40	0.23[c]– 0.36	0.62	651

[a] Free enzyme.

[b] Data from Engel and Dalziel [6].

[c] An approximation.

Table 3.2

NAD Region (mM)	$K^N_{m,\,app}$ (mM)	k^N_{app} (mole NADH/ mole e_f per min)
0.22 – 0.28	0.04	300
0.28 – 0.40	0.80	1 061
0.40 – 0.55	0.31	606
0.55 – 1.40	1.43	1 338

Table 3.3

Support Type	Loading (mg e_f/ g bead)	Linear Glu Region (mM)	Break Point (mM)	$K^G_{m,\,app}$ (mM)	k^G_{app} (mole NADH/ mole e_f per min)	$\Delta(K^G_{m,\,app}/k^G_{app})$ (μM Glu · mole e_f · min/mole NADH)
None[a]	—	0.40 – 1.40	none	0.17	596	0
CNBr-activated Sepharose	17.0	0.40 – 1.60	1.60	0.57	199	2.95
		1.60 – 10.0		1.69	291	
CNBr-activated Sepharose	2.8	0.50 – 10.0	none	1.45	668	0
CH-activated Sepharose	10.2	0.65 – 1.70	1.70	0.97	380	0.83
		1.70 – 10.0		1.69	502	
CH-activated Sepharose	4.9	0.50 – 1.60	1.60	0.91	289	2.03
		1.60 – 10.0		2.41	466	

[a] Free enzyme.

Figure legends

Fig. 3.1 pH activity profile of free (- - -) and immobilized (——) GluDH. The activity was assayed at 25°C in 87 mM sodium phosphate buffer containing 10 μM EDTA, 1 mM glutamate, 2 mM NAD, and either 0.9 –1.7 μg e_f/ml for immobilized GluDH or 2.5 –10.0 μg total protomers/ml for the free enzyme. The following GluDH preparations were analyzed: □, free GluDH; ○, 17.0 mg e_f/g CNBr-activated Sepharose; ×, 10.2 mg e_f/g CH-activated Sepharose; and △, 4.9 mg e_f/g CH-activated Sepharose.

Fig. 3.2 NAD activation of free GluDH at 25°C in 87 mM sodium phosphate buffer (pH 8.0) containing 10 μM EDTA and 50 mM glutamate. The enzyme concentration was 2.3 μg total protomers/ml.

Fig. 3.3 NAD activation of immobilized GluDH when 17.0 mg e_f (a) and 2.8 mg e_f (b) were each covalently bound to a gram of CNBr-activated Sepharose, or when 10.2 mg e_f (c) and 4.9 mg e_f (d) were each covalently bound to a gram of CH-activated Sepharose. The enzyme concentration was 0.6 – 1.7 μg e_f/ml in these experiments. All other experimental conditions were the same as those given in the legend of Figure 3.2. Only those data points connected by a solid line were used to calculate $K^N_{m,\,app}$ and k^N_{app} in Table 3.1. Dotted lines correspond to the regions given in Table 3.2.

Fig. 3.4 $v/[e_f]$ vs. [NAD] plot for immobilized GluDH (2.8 mg e_f/g CNBr-activated Sepharose). Experimental conditions were the same as those given in the legend of Figure 3.3.

Fig. 3.5 Glutamate inhibition of free GluDH at 25°C in 87 mM sodium phosphate buffer (pH 8.0) containing 10 μM EDTA and 2 mM NAD. The enzyme concentration was 0.72 μg total protomers/ml. Only those data points connected by a solid line were used to calculate $K^G_{m,\,app}$ and k^G_{app} in Table 3.3.

Fig. 3.6 Glutamate activation of immobilized GluDH. The following enzyme preparations were examined: □ , 17.0 mg e_f/g CNBr-activated Sepharose; ○, 2.8 mg e_f/g CNBr-activated Sepharose; ×, 10.2 mg e_f/g CH-activated Sepharose; and △, 4.9 mg e_f/g CH-activated Sepharose. The assay conditions were the same as those given in the legend of Figure 3.5 except that the GluDH concentration was 0.6 – 1.7 μg e_f/ml.

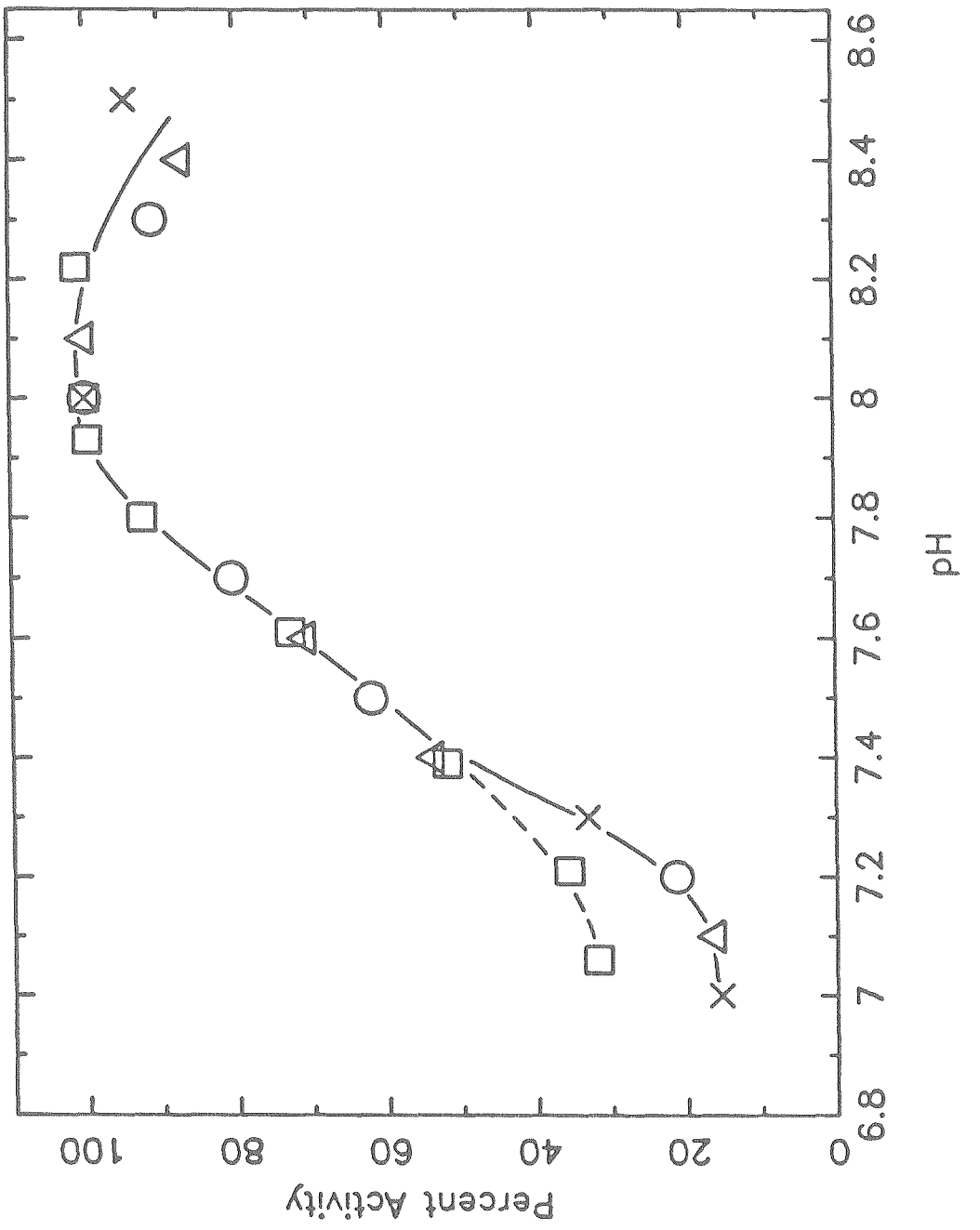

Figure 3.1

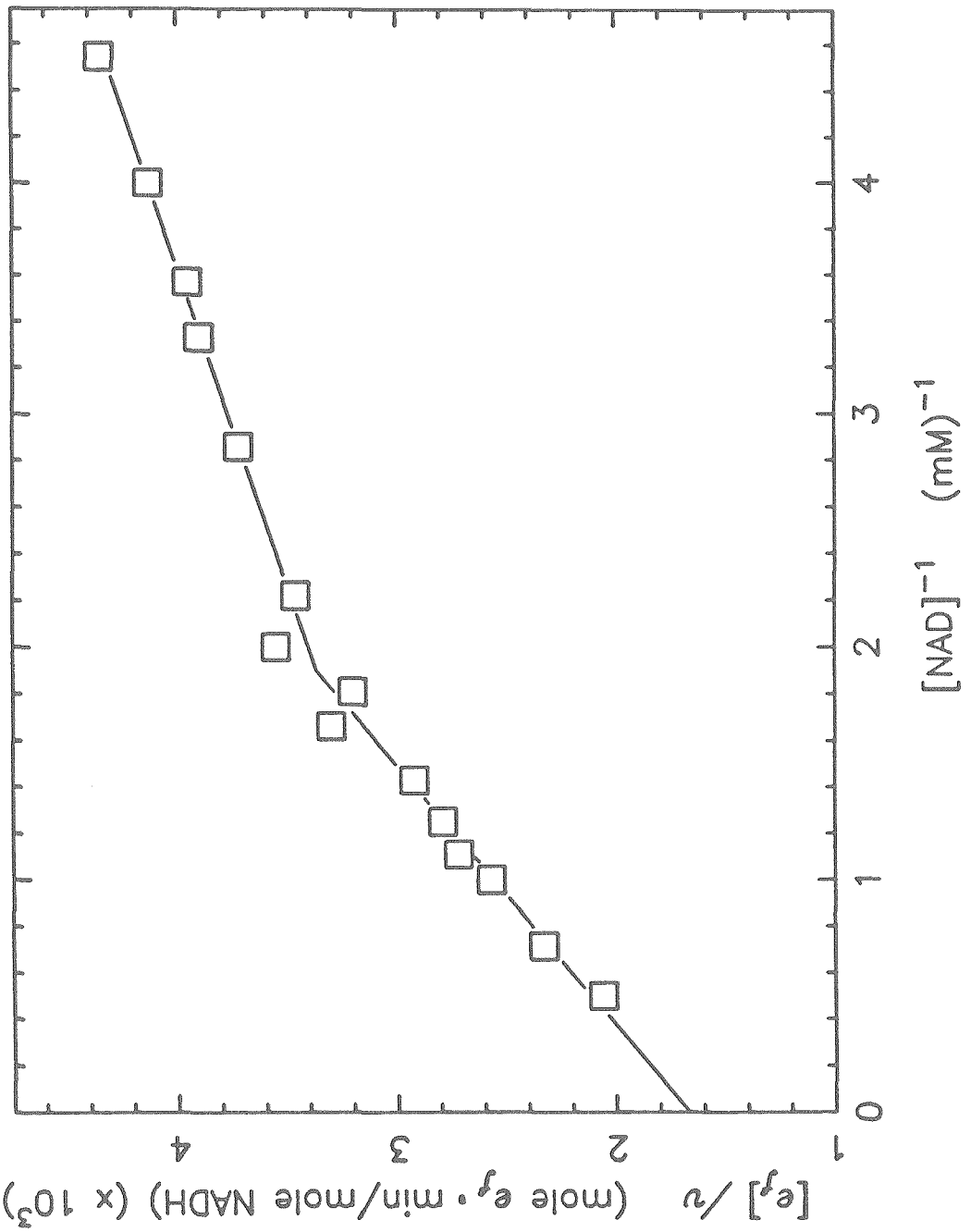

Figure 3.2

Figure 3.3

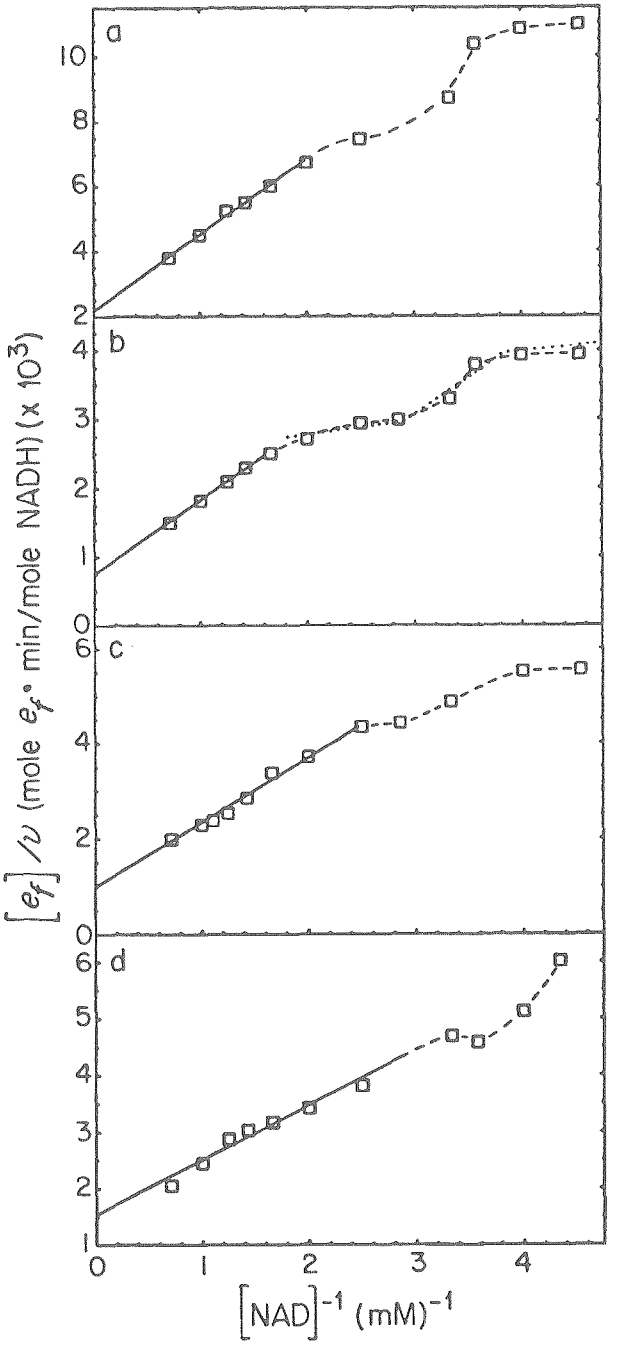

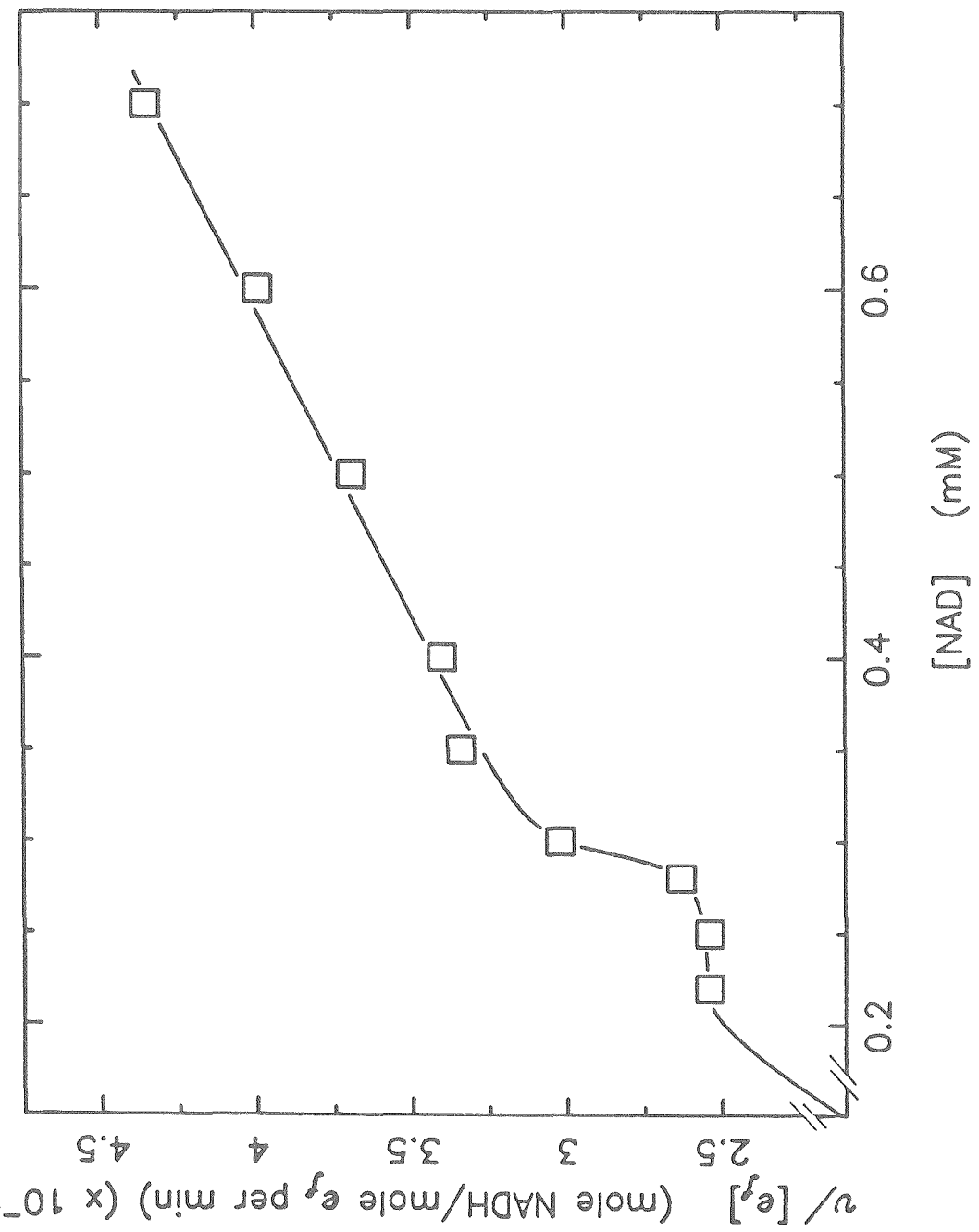

Figure 3.4

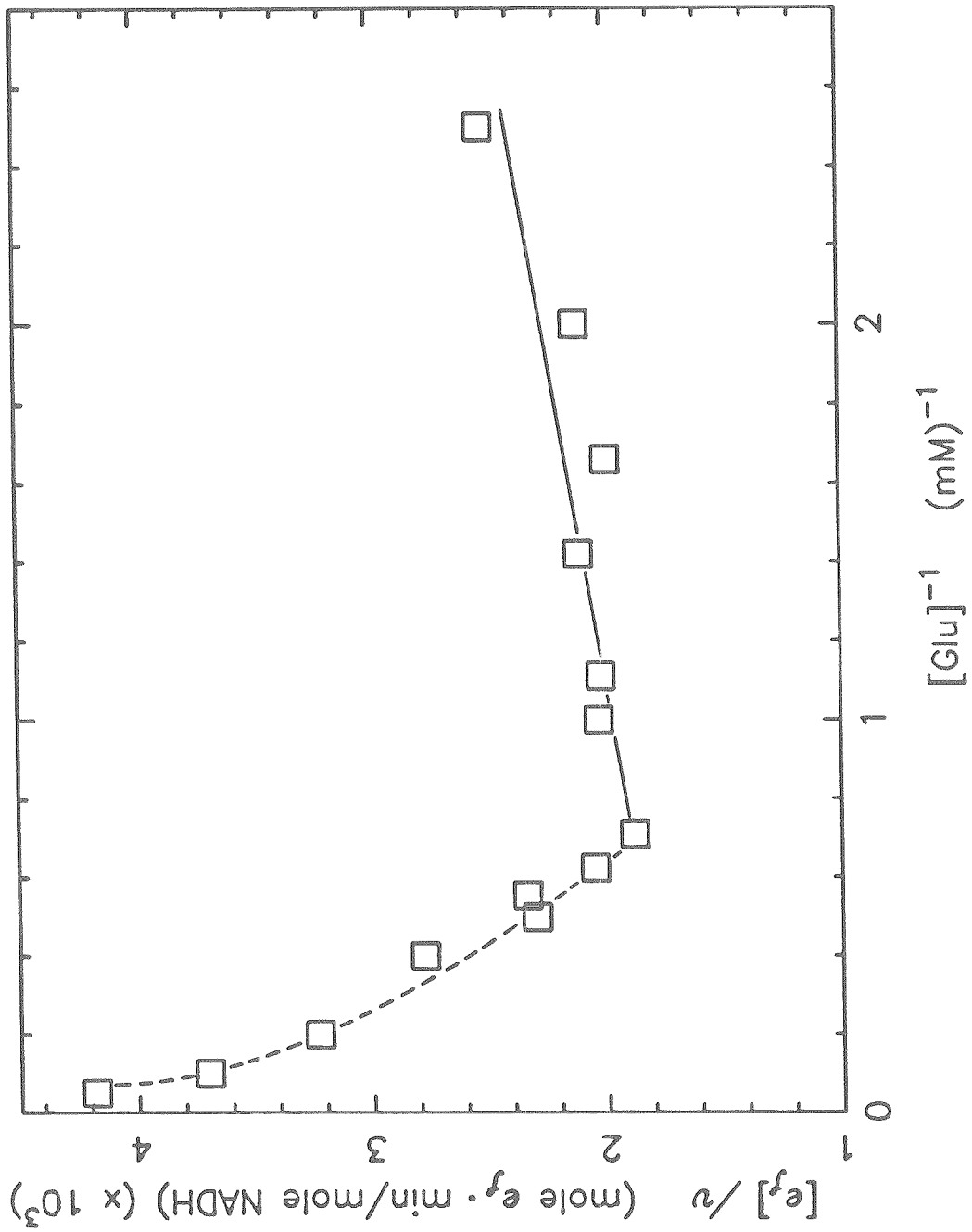

Figure 3.5

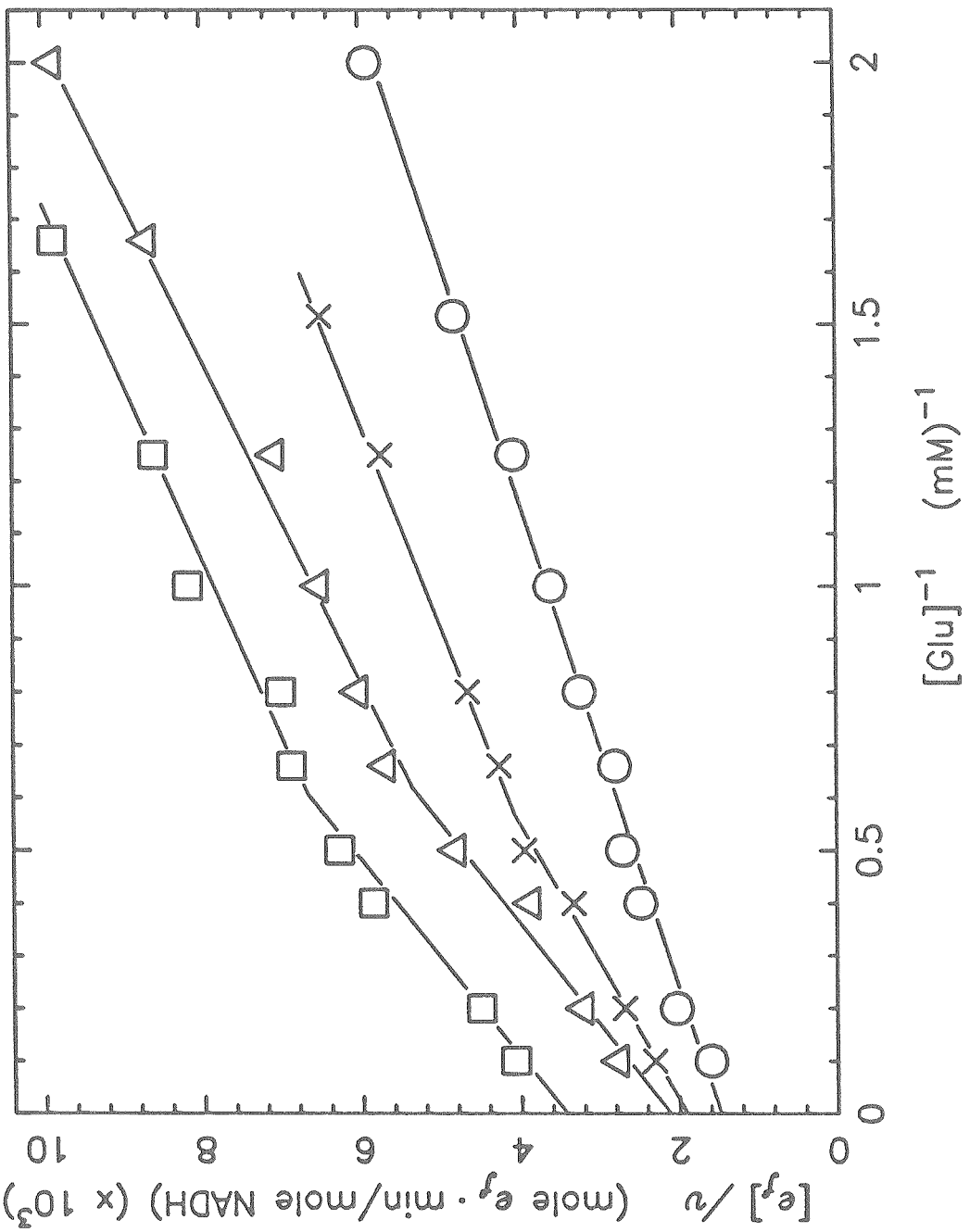

Figure 3.6

CONCLUDING REMARKS

The research presented in this work investigated free and immobilized bovine liver GluDH from both structural and kinetic perspectives. In this way, Sepharose-induced changes in GluDH structure and substrate activation, as well as the relationship between these two properties, was characterized. This was achieved by examining the structure of spin-labeled GluDH with ESR spectroscopy and by spectrophotometrically measuring the rate at which NAD deaminates glutamate. Specific conclusions from these structural and kinetic studies are summarized below. This is followed with a discussion on the implications of this research for other allosteric oligomers.

ESR spectra of ketone-labeled GluDH show that immobilization does not distort the structure of the enzyme; rather, it changes the distribution of ketone labels bound to two existing structures. This may represent a fundamental difference between immobilizing a monomer and an allosteric oligomer. Since GluDH undergoes conformational change, it may adopt the conformation which minimizes the strain imposed on it by immobilization. This suggests that the structure of a monomer with only one conformation would be distorted during immobilization. Previous studies with α-chymotrypsin demonstrate that this is the case.

A relationship between the percentage of ketone labels in population A, the more mobile spectral component, and the quaternary structure of the GluDH hexamer strongly suggests that the immobilized enzyme is structurally heterogeneous. Upon immobilization, two (or 33%) of the protomers in the GluDH hexamer may adopt a conformation different from that of the other four. If there are two binding sites for the ketone label per protomer, then this heterogeneity is reflected indirectly in the increased binding to these two protomers at

the secondary site. If there is only a single binding site per protomer, then the heterogeneity is reflected directly in the two structural conformations at this site.

Spin labeling free and immobilized GluDH with ClHgBz-TEMPO revealed that Sepharose-immobilization suppresses conformational change induced by GTP and NADPH and alters that induced by α-ketoglutarate. In addition, ESR spectra of immobilized GluDH containing at least two populations of mercuric labels that are bound to a single residue per protomer support the conclusion from the ketone-labeling experiments that the immobilized enzyme is structurally heterogeneous. The spectra of free and immobilized ClHgBz-TEMPO-GluDH are sufficiently compatible that the heterogeneity could exist in the free enzyme and be enhanced by immobilization.

Substrate-activation patterns are also affected by immobilization. NAD activation changes from being abrupt to being elongated and containing two inflection points. This pattern is the same for different loadings of GluDH on either CNBr- or CH-activated Sepharose 4B. Although the pattern of NAD activation is altered, the net effect of the activation is the same in both free and immobilized GluDH: it increases both $K^N_{m,\,app}$ and k^N_{app} (negative cooperativity). This information on NAD activation, as well as all other kinetic data presented in this thesis, is free of mass transport effects. The external effectiveness factor was unity, the observable Thiele modulus was less than $2.0 \cdot 10^{-4}$, and reaction-generated pH change was less than 0.01 during all kinetic experiments.

Upon immobilization, glutamate inhibition is replaced by activation. Glutamate activation of immobilized GluDH resembles NAD activation of the free enzyme. Both activations are abrupt and negatively cooperative. The intensity

of the Sepharose-induced activation, $\Delta(K^G_{m,\,app}/k^G_{app})$, is inversely related to the apparent rate constant. Moreover, glutamate activation only occurs in those immobilized GluDH preparations that have k^G_{app} values that are less than the apparent rate constant for the free enzyme, 596 mole NADH/mole e_f per min.

A comparison of the substrate activation properties from this and other studies of GluDH suggests that these properties exist in free GluDH and are magnified by immobilization. Engel's and Ferdinand's kinetic model of NAD activation of the free enzyme predicts a pattern of change in kinetic activity and substrate binding similar to that shown in Table 3.2. Hornby and Engel reported that free GluDH is abruptly activated by analogs of glutamate. Furthermore, the activation is negatively cooperative and the correlation between $\Delta(K^G_{m,\,app}/k^G_{app})$ and k^G_{app} is valid in Hornby's and Engel's system.

Several free oligomers have activation properties similar to those of immobilized bovine liver GluDH: *E. coli* CTP synthetase, *E. coli* W phosphoenolpyruvate carboxylase, honeybee glyceraldehyde 3-phosphate dehydrogenase, *E. coli* B ADP-glucose pyrophosphorylase and *Blastocladiella emersonii* GluDH. All have elongated activation regions containing two inflection points. Teipel's and Koshland's model predicts that this type of activation corresponds to changes in the binding and rate constants similar to those shown in Table 3.2.

Results from the structural and kinetic studies of GluDH suggest that structural heterogeneity and conformational change are related to substrate activation. First, Teipel's and Koshland's, as well as Engel's and Ferdinand's, kinetic model predicts that these structural properties could cause activation. Second, ESR spectra of GluDH modified with either the ketone or mercuric label indicate that the immobilized enzyme is structurally heterogeneous. Moreover,

these spectra suggest that, perhaps, this heterogeneity is present in the free enzyme and is magnified by immobilization. This magnification parallels the Sepharose-induced change in substrate activation: on the whole, the activation patterns are present in the free enzyme, but they are less pronounced. Third, ESR spectra of ClHgBz-TEMPO-GluDH reveal that immobilization restricts one type of conformational change while modifying another. Previous kinetic and spectroscopic studies of GluDH suggest that conformational change is related to activation. The fact that immobilization affects both conformational change and activation indicates that the relationship between the two is valid. Finally, three of the free oligomers which have activation properties similar to those of Sepharose-immobilized GluDH undergo conformational change or exist in two structural forms that can be physically separated.

In summary, Sepharose-immobilization exaggerates both structural and kinetic properties of GluDH that are present in the free enzyme. More research is needed to determine if this is a general feature of immobilized oligomers. If this is the case, then, possibly, immobilizing conditions can be chosen to enhance a specific property of the oligomer that is desirable for a particular industrial or medical application. In addition, the investigation of structure-function relationships was facilitated by the exaggerated properties of the immobilized enzyme. In the future, ESR spectroscopy could be employed to study allosteric regulation in those free oligomers described in this thesis which exhibit activation patterns similar to those of immobilized GluDH.